Electrospinning of pullulan-based orodispersible films containing sildenafil

Elisabetta Ravasi[1], Alice Melocchi[2], Alessia Arrigoni[1], Arianna Chiappa[1], Chiara Grazia Milena Gennari[2], Marco Uboldi[2], Chiara Bertarelli[1], Lucia Zema[2,*] and Francesco Briatico Vangosa[1,*]

[1]Dipartimento di Chimica, Materiali e Ingegneria Chimica "G. Natta", Politecnico di Milano, Piazza Leonardo da Vinci 32, 20133 Milano, Italy

[2]Sezione di Tecnologia e Legislazione Farmaceutiche "Maria Edvige Sangalli", Dipartimento di Scienze Farmaceutiche, Università degli Studi di Milano, via Giuseppe Colombo 71, 20133, Milano, Italy

*Correspondence: lucia.zema@unimi.it (L.Z.) francesco.briatico@polimi.it (F.B.V.)

Keywords: fast-dissolving, pediatric patients, nanofibers, drug delivery, natural polymer, green pharmaceutics, rheology.

Abstract

Feasibility of electrospinning in the manufacturing of sildenafil-containing orodispersible films (ODFs) intended to enhance oxygenation and to reduce pulmonary arterial pressure in pediatric patients was evaluated. Given the targeted subjects, the simplest and safest formulation was chosen, using water as the only solvent and pullulan, a natural polymer, as the sole fiber-forming agent. A systematic characterization in terms of shear and extensional viscosity as well as surface tension of solutions containing different amounts of pullulan and sildenafil was carried out. Accordingly, electrospinning parameters enabling the continuous production, at the highest possible rate, of defect-free fibers with uniform diameter in the nanometer range were assessed. Morphology, microstructure, drug content and relevant solid state as well as ability of the resulting non-woven films to interact with aqueous fluids were evaluated. To better define the role of the fibrous nanostructure on the performance of ODFs, analogous films were produced by spin- and blade-coating and tested. Interestingly, the disintegration process of electrospun products turned out to be the fastest (*i.e.* occurring within few s) and compliant with Ph. Eur. and USP limits, making relevant ODFs particularly promising for increasing sildenafil bioavailability, thus lowering its dosages.

1.Introduction

In the last decades, the implementation of innovative manufacturing processes in the pharmaceutical field has represented a promising development strategy, especially at the research level. Indeed, such an approach was demonstrated useful not only to reduce production costs, but also to favor the development of drug delivery systems (DDSs) having unique design and performance characteristics. This was the case of hot melt extrusion, injection molding, 3D and 4D printing as well as of electrospinning [Andreadis et al., 2022; Kallakunta et al., 2019; Madruga et al., 2022; Melocchi et al., 2021; Sarabu et al., 2019; Zema et al., 2012, 2017]. Notably, the latter process is driven by a high voltage electric field that, starting from polymeric solutions, suspensions and melts, enables the fabrication of an inter-connected web, often named as non-woven mat, composed of long and uniform micro- and nano-fibers [Cleeton et al., 2019; Laudenslager et al., 2012; Ramakrishna et al., 2005]. The electrospinning technology stands out for its ease of operation, cost-effectiveness and scalability [Guo et al., 2022; Persano, et al., 2013; Si et al., 2023]. Moreover, given the reduced diameter and high surface-to-volume ratio the resulting fibers are provided with, they have found application in many different areas, such as tissue engineering, biosensors, water filtration and wound dressings [Hassan et al., 2020; Luraghi et al., 2021; Xu et al., 2023; Zhan et al., 2022].

When applied to pharmaceutics, electrospinning was employed for the fabrication of systems mainly intended for transdermal delivery and implantation [Ignatova et al., 2013; Kumar et al., 2021; Meinel et al., 2012]. Indeed, the similarity between electrospun fibers and the natural fibrillary extracellular matrix turned out to facilitate attachment and proliferation of cells when tissue regeneration is pursued [Doostmohammadi et al., 2020; Gao et al., 2019]. At the same time, in view of their high surface area, non-woven mats attained by electrospinning were deemed interesting as orodispersible films (ODFs) for oral administration of drugs [Balusamy et al., 2020; Ignatious et al., 2010]. Such films appear as strips of thin polymeric layers to be placed onto the tongue and are intended to disintegrate/dissolve almost instantaneously in the saliva, thus not requiring water or swallowing [He et al., 2021a; Hoffmann et al., 2011; Preis et al., 2013]. Thanks to this unique behavior, ODFs may enhance therapy adherence in the case of pediatric and geriatric subjects, as well as of people affected by dysphagia, Parkinson's disease or mucositis [Scarpa et al., 2017; Slavkova et al., 2015]. Being the active ingredient expected to dissolve quickly, ODFs might also provide a faster onset of action and improved bioavailability with respect to other oral products. Indeed, if drug absorption mainly occurs through the oral mucosa, first-pass metabolism would be prevented [Ferlak et al., 2023; Visser et al., 2017]. In addition, ODFs are known to provide accurate and flexible dosing, being in principle able to fulfil the raising needs of precision medicine. So far, they were mainly fabricated by either solvent casting and hot melt extrusion but, more recently, preliminary data on their feasibility *via* 3D

printing were also collected [Gupta et al., 2021; Khalid et al., 2021a,b; Musazzi et al., 2020]. When applied to ODFs manufacturing, the electrospinning process could lead to products with intrinsic high porosity, so as with improved performance, while avoiding the need for post-processing steps, such as drying or cooling, thus containing overall production costs [Kean et al., 2023].

Independent of the manufacturing process considered, film-forming polymers are essential components of ODFs. In the last years, new materials, for instance derived from the food industry, has started to be considered, with particular attention towards gluten-free, preservative-free polymers of vegetable origin [Garsuch et al., 2010; George et al., 2019; Ngwuluka et al., 2014]. In this respect, pullulan could represent an interesting candidate [Badhwar et al., 2018; Leathers et al., 2003; Singh et al., 2017]. It is a linear homopolysaccharide, synthesized by a yeast-like fungus through a fermentation process, and consists in maltotriose units (*i.e.* three glucoses connected by α-1,4 glycosidic bonds) linked to each other by an α-1,6 glycosidic bond. Such a peculiar pattern provides this polymer with high structural flexibility and enhanced solubility characteristics. Moreover, pullulan shows good adhesive properties and is able to form strong, oxygen impermeable films. While electrospinning potential of pullulan have started to be investigated especially in food packaging, only few similar studies were carried out in the drug de-livery field and even less targeted the production of ODFs [Chachlioutaki et al., 2020; Ponrasu et al., 2021; Qin et al., 2019; Sun et al., 2012]. In these articles, pullulan was mainly proposed as an electro-spinnability adjuvant, being able to raise the viscosity of the feedstock formulations based on other polymers, while lowering relevant conductivity as well as surface tension.

Based on these premises, the aim of the present work was to preliminarily evaluate the feasibility of electrospinning in the manufacturing of pullulan-based ODFs intended for the administration of sildenafil to pediatric patients. Indeed, sildenafil was recently proven useful in the treatment of persistent pulmonary hypertension in newborns and children, improving oxygenation index and pulmonary arterial pressure [Dhariwal et al., 2015; Evers et al., 2021; He et al., 2021b; Li et al., 2021; Zhang et al., 2020]. In this respect, oral administration of 0.1 to 0.5 mg/kg every 8 h was recommended, eventually customizing the dosing regimen based on therapy response [Abman et al., 2015]. However, the drug is subjected to a marked first-pass metabolism and for this reason would benefit greatly from buccal absorption [Nichols et al., 2002]. Given the targeted patients, the use of a natural polymer was considered essential, spinning adjuvants were avoided and water was selected as the only solvent. A systematic evaluation of pullulan-based placebo and drug-containing formulations to be electrospun was first carried out, followed by the selection of appropriate processing conditions and the manufacturing of ODF prototypes to be characterized.

2. Materials and Methods

2.1. Materials

Sildenafil citrate (A.C.E.F., I): solubility in water = 4.1 ± 1.3 mg/mL [Ouranidis et al., 2021]; pullulan 300kDa (n° batch 9F21, Hayashibara Co. Ltd., J). All solvents were of analytical grade unless specified.

2.2. Methods

2.2.1. Preparation of the solutions

Placebo and drug-containing solutions were prepared varying the concentration of both pullulan and sildenafil citrate. A pre-determined volume of distilled water was added to an accurately weighted amount of pullulan (analytical balance, AS310.R2, RADWAG, P). Specifically, the polymer quantity was calculated as weight percentage (%wt) with respect to the overall solution weight, resulting in formulations containing 10, 15 and 20%wt of pullulan. These percentages were well-above the critical concentration for entanglements (*i.e.* ~ 6 %wt), as their presence was expected to foster the spinnability of the resulting solutions [Qi et al., 2009]. Drug solubility in water at ambient conditions (*i.e.* 25.0 °C) was determined, resulting in 3.5 mg/mL. Drug-containing formulations in the 2‰-3.5‰wt range were prepared from a supersaturated water-based stock solution of sildenafil citrate. This was progressively diluted to attain solutions with the desired drug concentrations, which were then used to dissolve pullulan. All the formulations were gently stirred overnight to promote complete pullulan dissolution while preventing degradation phenomena of the polymer chains due to excessive stresses.

2.2.2 Characterization of the solutions

2.2.2.1 Shear viscosity

Measurements of the steady state shear viscosity were carried out using a Modular Compact Rheometer (MCR 502, Anton Paar GmbH, AT) equipped with a cone-plate geometry (ø = 50 mm, angle 1 deg, truncation 99 μm). The instrument worked under controlled shear rate mode, with shear rate ranging between 1 and 1000 s^{-1}. A Peltier plate and a hood system allowed to control the temperature and to limit possible water evaporation. All experiments were performed at 25.0 °C. For each formulation, five samples were characterized, reporting the results in terms of mean viscosity and relevant standard deviation.

2.2.2.2 Extensional viscosity

Extensional behavior of the solutions was studied by Capillary Breakup Rheometry (CaBeR). According to this technique, a stepwise uniaxial extensional flow was imposed to a fluid filament, estimating its rheological properties from the reduction in relevant diameter over time. More into detail, the solution to be tested is placed between two parallel plates positioned at a certain distance (L_0) representing the so-called initial gap. The plates are then rapidly pulled apart to a final distance (L_1), named final gap, thus generating an hourglass shaped liquid filament. After the initial plates motion, no further external stretch is imposed to the liquid. Due to the generated curvature, surface tension acts as a pinching force, causing the evolution of the hourglass liquid into a filament that thins up to rupture. Changes in filament radius, measured on the filament symmetry plane (Rmid), allow to estimate either the extensional viscosity or the longest relaxation times for viscous and viscoelastic fluids, respectively [Anna et al., 2001; Entov et al., 1997].

The experiments were performed at ambient conditions (*i.e.* 25°C) using an HAAKE CaBeR1 (Thermo Fisher Scientific, Karlsruhe, D) Capillary Breakup Rheometer, equipped with 6mm plates. Before the step stretch, the plate distance was set at 3 mm, while the applied nominal Hencky strain ($\hat{\varepsilon}_H$ was equal to 0.91 and calculated as follows:

$$\hat{\varepsilon}_H = \ln\frac{L_1}{L_0} \qquad \text{(Eq. 1)}$$

R_{mid} was measured by means of the laser micrometer the CaBeR1 apparatus was provided with. Moreover, the whole filament shape was monitored during testing to rule out possible instabilities, such as beads formation. For this purpose, a high-speed megapixel CMOS camera Mikrotron MC1310 (Mikrotron GmbH, Unterschleissheim, D) equipped with Computar MC TV lens characterized by a focal length of 50 mm was employed. Images were acquired at 500 fps or 1000fps rate with a 1000 x 1000 pixel resolution. For each formulation, five samples were characterized, reporting the results in terms of mean viscosity and relevant standard deviation.

2.2.2.3 Surface tension

The surface tension was studied by testing 10 drops for each solution with the pendant drop method, by means of a Dataphysics OCA 15plus tensiometer (DataPhysics Instruments GmbH, D) All measurements were taken at ambient conditions (*i.e.* 25 °C) using a 500 μL Hamilton syringe and a needle of 1.83 mm in diameter. The drop shape was observed through a charge coupled device camera and analyzed to infer the surface tension via the SCA 20 Dataphysics software, taking advantage of

the solution nominal density data. For each formulation, five samples were characterized, reporting the results in terms of mean viscosity and relevant standard deviation.

2.2.3 Preparation of ODFs by electrospinning

Electrospinning was carried out in an in-house assembled unit. The feeding solution was loaded into a 2.5 mL syringe, on which a 15-gauge needle was mounted (Hamilton Gas tight model 1000 TLL, D). The syringe was positioned into a mobile infusion pump (KDS Scientific, model series 200, I), which fed the polymeric solution into the capillary nozzle at a constant flow rate. A high voltage power supply (Spellman SL30P300, I) was connected to the needle to provide the driving potential, while the collector was grounded. Both glass and aluminum plates were used. Spinning was carried out in horizontal and vertical (bottom to top) directions. Spinning temperature and humidity ranged between 21 °C and 24 °C and 20% and 50% RH, respectively. Feed rate and electric potential difference were varied in the range 0.1 - 6 mL / h and 15 - 21 kV, respectively.

Electrospinning parameters were selected as described in the Results and Discussion Section, in order to attain uniform nanofibers, in the form of non-woven films, at the highest possible spinning rate.

Aspect and diameter of resulting fibers were assessed through optical (Olympus B60 with camera Infinity 2, magnifications from 5x to 100x) and scanning electron (Environmental SEM Zeiss EVO 50 EP) microscopy. In the latter case, samples were laid on a metal stub, coated with thin layer of gold and then observed in high vacuum conditions.

2.2.4 Preparation of ODFs by coating techniques

Compact films were manufactured by either spin- or blade-coating starting from the same solutions used for electrospinning.

For spin-coating, placebo and drug-containing pullulan-based solutions were dripped on a glass collector spinning first at 3000 rpm for 1 min 30 s and then at 500 rpm for 30 s (Spin Coater, model WS−400B−6NPP/lite, Laurell Technologies, US-PA). After solvent evaporation, free films were collected. During blade-coating, the above mentioned solutions were poured on a suitable substrate, spread at a fixed rate of 3 mm/s by a blade and then dried to remove water (K Control Coater, RK Print Coat Instruments Ltd., UK). Suitable substrates for placebo and drug-containing solutions were glass and aluminum, respectively.

Blade-coated films were kept 2h at ambient condition within a glass desiccator containing silica, to slow down solvent evaporation at the beginning of the drying process, so as to prevent the formation

of air bubbles. Then, the films were placed in a climatized room maintained at 25 ± 1 °C, RH within 21-53%, to reach the moisture equilibrium, which overall required approximately 3 h.

2.2.5 Physico-technological characterization of films

All the films produced were characterized for weight (analytical balance, AS310.R2, RADWAG, P) and thickness, which was measured in five different points along each sample (n = 6; IP65 0-25mm, Mitutoyo, J).

2.2.6 Drug content

Drug content was determined on both solutions and resulting films via high performance liquid chromatography (HPLC) (Chemstation, Agilent Technologies, I). The latter was equipped with an UV-Vis detector and a L-column 150 x 4.6 mm InertCloneTM 5µm ODS(3) 100Å (Phenomenex, US-MA). The mobile phase (flow rate = 1 mL/min at 30 °C) was composed of acetonitrile, methanol and an aqueous solution containing 0.7% v/v triethylamine (pH = 3 ± 0.1 adjusted using phosphoric acid) (composition 17 / 25 / 58% by volume). Before the analyses, approximately 10 mg of each solution to be tested was accurately weighted and diluted up to 20 mL, with the aqueous solution employed for the preparation of the mobile phase. 2 mL of the latter were also used to dissolve previously weighed film specimens (analytical balance, Gibertini, I).

Aqueous solutions to be analyzed were transferred in appropriate HPLC vials and automatically injected (20 µL, 30 °C) into the equipment for being assayed spectrophotometrically (retention time = 11 min; λ = 290 nm). The drug concentrations were determined using a calibration curve purposely built in the 0.55-55 µg/mL range (R^2 = 0.998).

2.2.7 FT-IR Spectroscopy

The IR absorption spectra were recorded using a Nicolet NEXUS FT-IR spectrometer (4 cm^{-1} resolution, 128 scans) (Thermo Fisher Scientific, US-MA) equipped with a Thermo-Electron Corporation Continuum FT-IR microscope. While powder samples were tested in transmission mode using a Diamond Anvil Cell (DAC) accessory, films were analyzed in ATR mode using a Si tip single bounce ATR accessory.

2.2.8 *In vitro* disintegration test

Disintegration (n = 6) was tested according to *i)* the Ph. Eur. ("Disintegration of tablets and capsules"), *ii)* the USP ("Procedure for uncoated or plain-coated tablets") and *iii)* a method purposely setup and based on the available ODFs-related literature [Garsuch et al., 2010; Ponrasu et al., 2021; Saab et al., 2019]. In this respect, a film sample previously weighted (analytical balance, Gibertini, I) was dropped onto a petri dish (ø = 60 mm) filled with 4 mL of distilled water, which was kept at 37± 0.5 °C. A 15 mm x 15 mm. Then, 2 mL of distilled water (kept at 37 ± 0.5 °C) were added on top of the film with a syringe. During the trial, the behavior of the sample was recorded using either *i)* a Mikrotron MC1310 (Mikrotron GmbH, D) 1 megaPixel CMOS high-speed camera (acquisition rate 300 fps), equipped with Computar MC TV lens characterized by a focal length of 50 mm, or *ii)* a UI1490LE-M-GL (IDS imaging, Obersulm, D) Ueye camera (acquisition rate 3 fps), equipped with Computar MACRO 10× lens (Tokyo, J), respectively.

3. Results

The first aim of the work was to identify electrospinning conditions leading to the production of good quality nanofibers, in the form of non-woven films, at the highest possible drug concentration and spinning rate, starting from the simplest formulation consisting in a pullulan-based aqueous solution containing sildenafil. As structure, diameter and morphology of electrospun fibers are well-known to depend not only on the process parameters (*e.g.* voltage, temperature, pressure, flow rate) but also on rheological behavior, conductivity and surface tension of the feedstock formulation employed, preliminary studies were carried out in this respect.

3.1. Physico-chemical characterization of pullulan/sildenafil solutions and selection of the formulation to be electrospun

The rheological behavior in shear of aqueous solutions containing different amounts of pullulan, either alone or with sildenafil, was first investigated. While for drug-containing formulations the saturated solution represented the starting point, attaining lower concentrations by dilution, the pullulan content was varied between 10 and 20%. In this respect, accuracy of the dilution process was verified, confirming the correspondence with the nominal drug content.

Viscosity (η) versus shear rate ($\dot{\gamma}$) profiles were built and fitted with the Cross equation:

$$\frac{\eta}{\eta_0} = \frac{1}{1+(\lambda\dot{\gamma})^{\mathrm{m}}} \qquad \text{Eq. (2)}$$

in which η_0 represents the zero shear viscosity, λ a relaxation time and m an index of the shear thinning tendency. By way of example, shear viscosity curves relevant to solutions based on the polymer as such and saturated with sildenafil are reported in Figure 1, together with experimental data fitting. Values of the above-mentioned fitting parameters (*i.e.* η_0, λ and m) are reported in Figure 2 as a function of the amount of pullulan. As expected, higher pullulan contents resulted in increased η_0 and λ values, but determined a very slight decrease in the shear thinning behavior of the formulations. A very small tendency towards viscosity reduction was shown by the polymeric solutions saturated with sildenafil, irrespective of the pullulan concentration. Notably, a similar effect was visible even reducing the drug amount (Supplementary material, Figure S1). However, no major interactions between the active ingredient and the polymer were revealed by shear rheology.

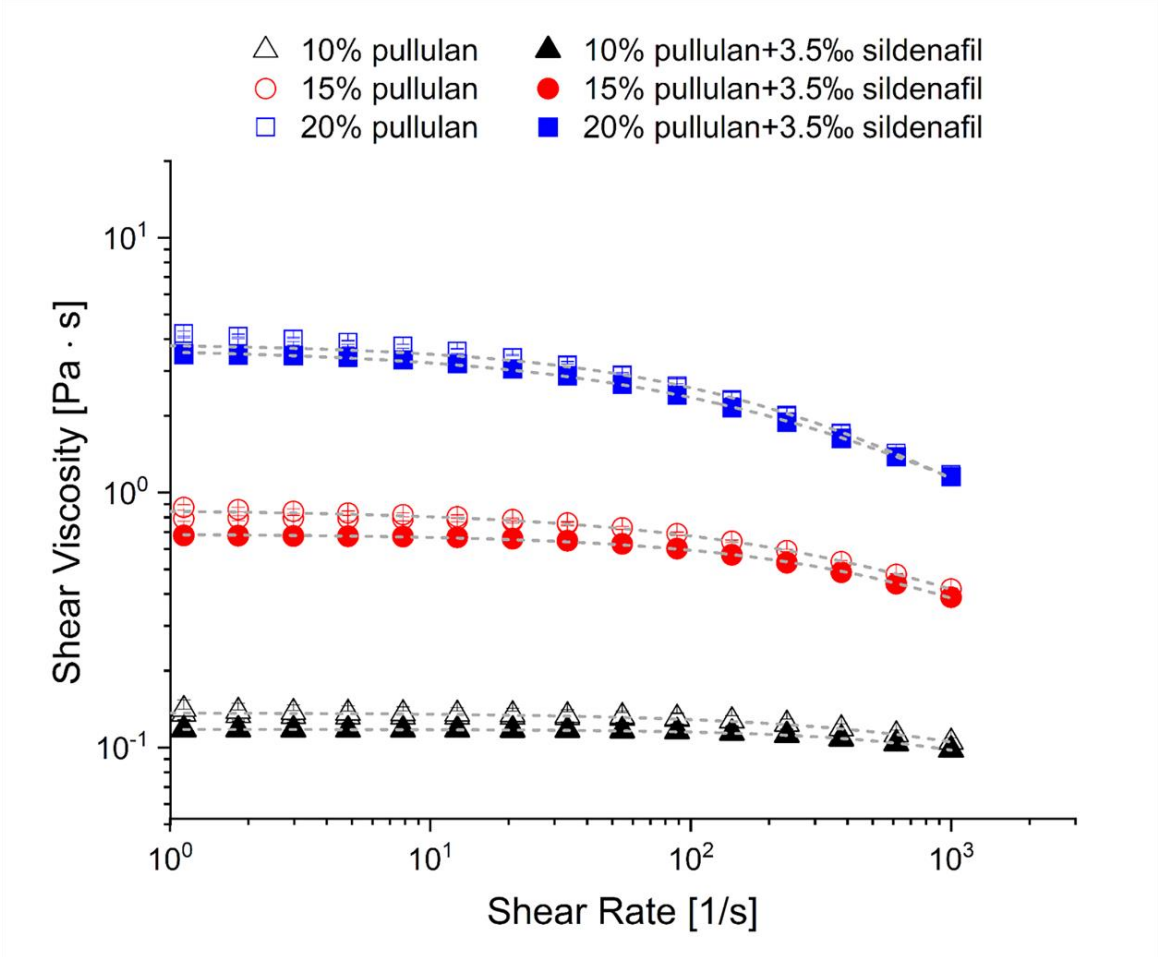

Figure 1: viscosity curves relevant to pullulan-based solutions containing either the polymer as such or with sildenafil. Dashed lines represent experimental data fitting with the Cross model.

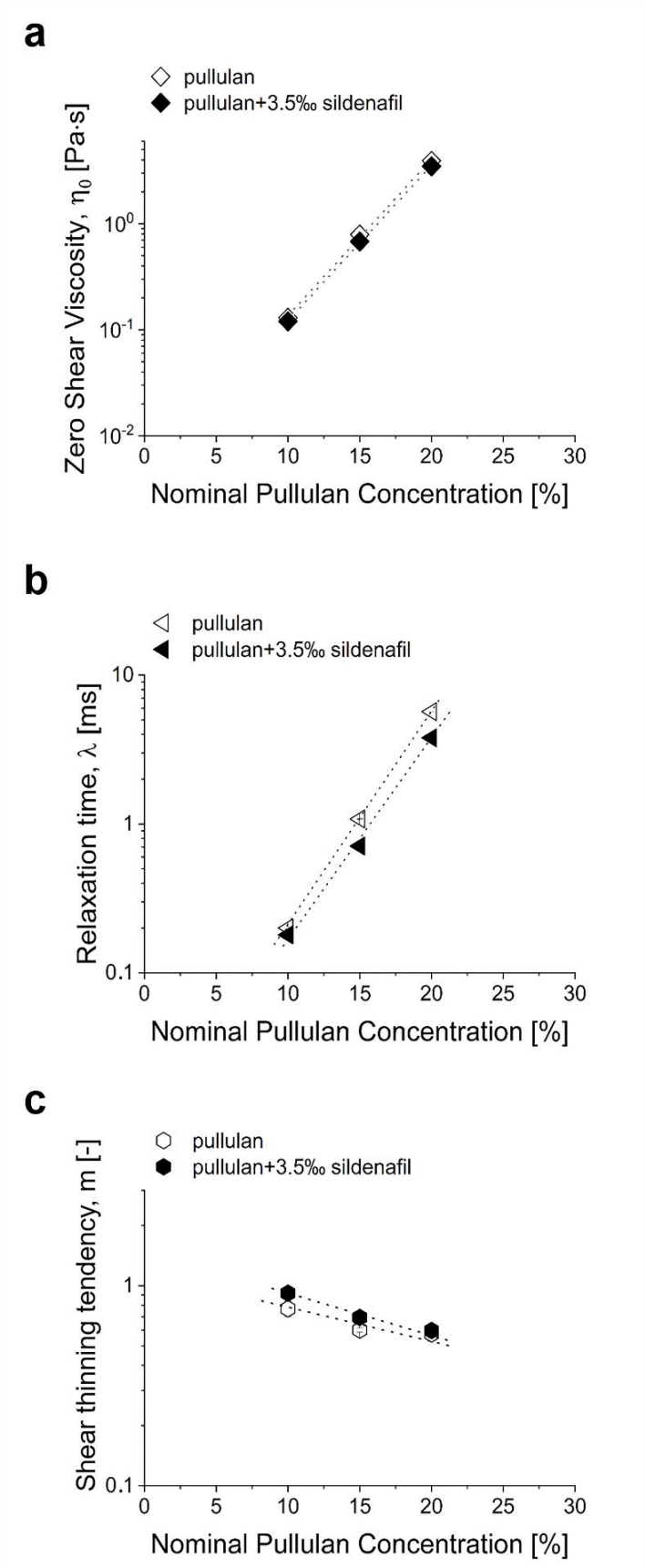

Figure 2: a) zero shear viscosity, b) relaxation time and c) shear thinning index versus pullulan concentration in the solutions containing either the polymer as such or with sildenafil. Dotted lines should be intended as a guide to the eye.

Extensional viscosity tests were also performed with a Capillary Breakup Rheometer (Figure 3). After a sudden thinning occurring during plates motion, in the first few milliseconds of testing three regimes could be recognized controlled by: *i)* the competition of capillary (*i.e.* surface tension and curvature generated) forces and fluid inertia, *ii)* the viscosity of the solution and *iii)* the (visco)elasticity of the latter [McKinley et al., 2022; Verbeke et al., 2020]. Fitting the data relevant to the final part of the curves (*i.e.* when the viscoelastic response of the solutions starts dominating the breakup phenomenon and slows down the filament thinning) with the Hentov and Hinch equation, the longest relaxation time was estimated as:

$$\frac{D(t)}{D_0} = \left(\frac{D_0 G}{4\sigma}\right)^{1/3} \exp\left(-\frac{t}{3\lambda_c}\right) \qquad \text{Eq. (3)}$$

in which D(t) and D_0 are current and initial filament diameter, G is the shear modulus of the elastic material, σ represents the surface tension and λ_c a relaxation time. To better appreciate the changes undergone by the filament diameter over time, photographs taken during the experiments were also added to Figure 3.

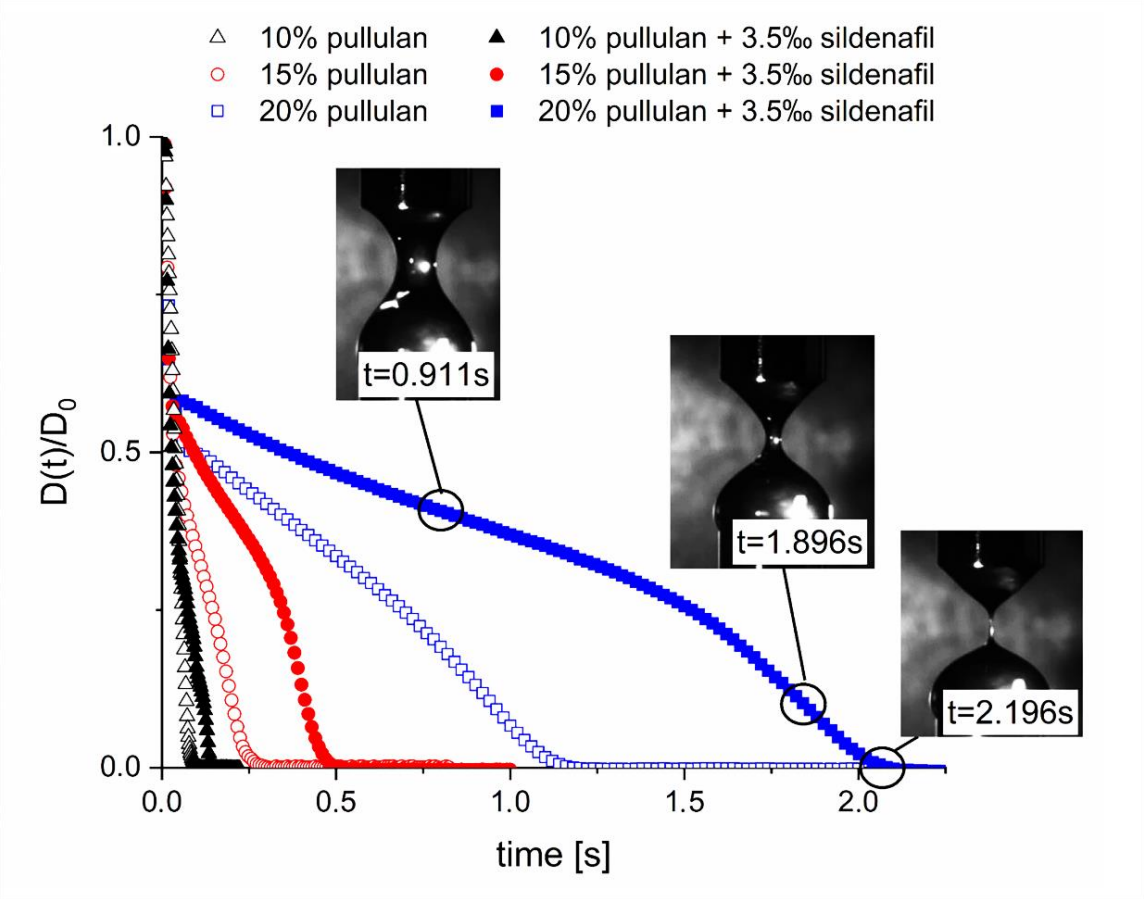

Figure 3: changes in filament diameter over time during capillary breakup experiments. The diameter (D) was measured on the symmetry cross-section of the filament and was normalized using the plate diameter (D_0 = 6mm). By way of example, some photographs taken during the experiment are included.

Estimated relaxation times and time to breakup values, the latter being evaluated from diameter versus time curves reported in Figure 3, were then plotted versus the amount of pullulan contained in the placebo and drug-containing solutions (Figure 4).

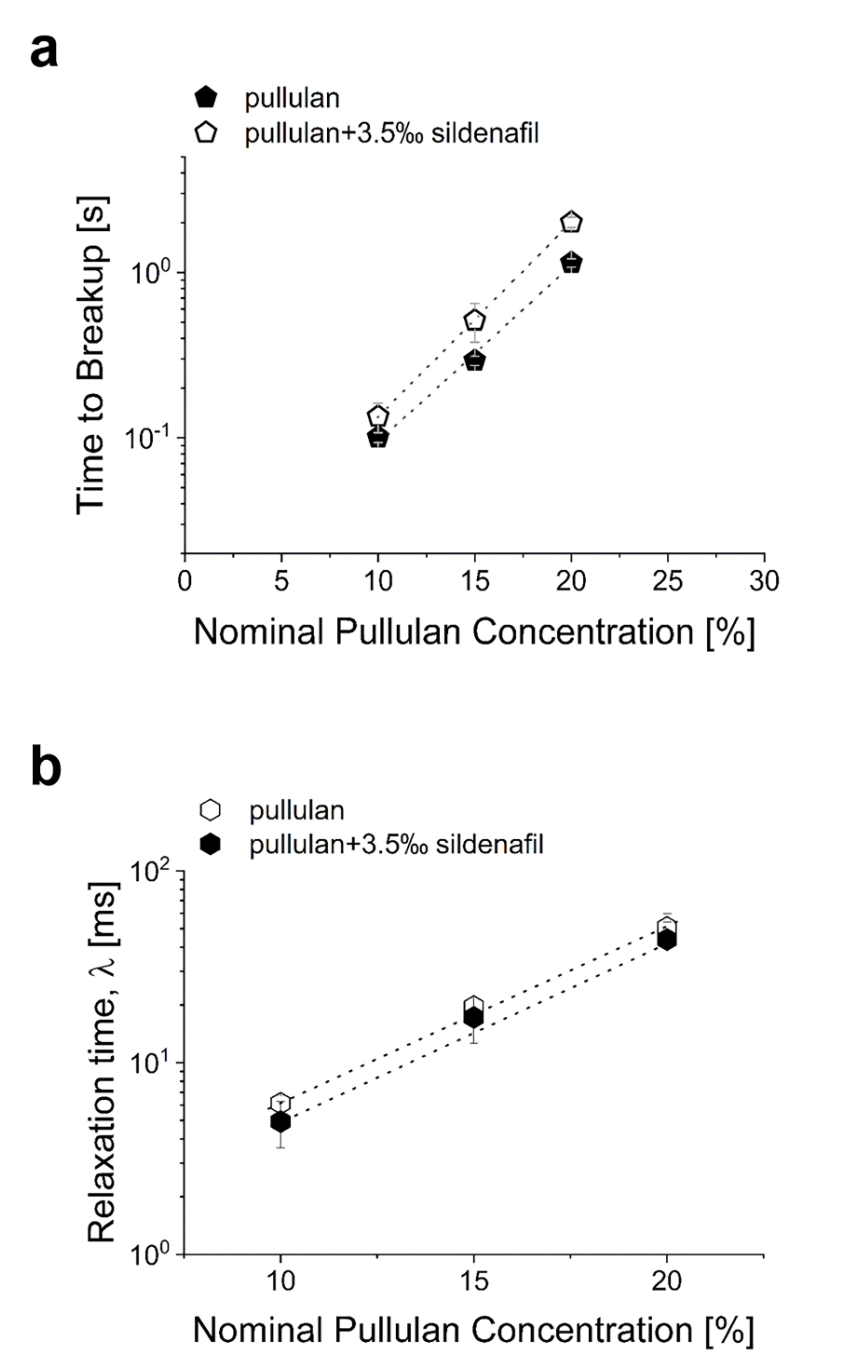

Figure 4: a) time to breakup and b) relaxation time versus pullulan concentration in the solutions containing either the polymer as such or with sildenafil. Dotted lines are intended as a guide for the eye.

As expected, increasing the pullulan concentration and, as a consequence, the viscosity of the relevant solution, the time needed for the liquid filament to breakup turned out longer. On the other hand, the presence of sildenafil affected the rate of this phenomenon, causing the breakup to occur relatively later (Figure 4a). As before observed during tests performed in shear, the relaxation time increased with pullulan concentration, and, dealing with formulations having the same polymeric content, this

parameter tended to be slightly reduced by the presence of sildenafil (Figure 4b). The decrease in relaxation time as well as in shear viscosity observed with pullulan solutions due to the presence of the drug could be associated with a lower resistance to filament stretching and should thus bring to a shorter filament lifetime, although this would be inconsistent with the tendency pointed out by time to breakup data. However, filament thinning was driven by the capillary action of solution surface tension, which was significantly decreased by the presence of the active ingredient, regardless of the polymer amount of the solution under investigation (Figure 5a). Furthermore, such a reduction was shown to depend on sildenafil concentration (Figure 5b). In this respect, it was hypothesized that the increase in time to breakup highlighted by solutions containing sildenafil could be due to a reduction in the driving force, which compensate the (indeed limited) decrease in viscoelastic resistance.

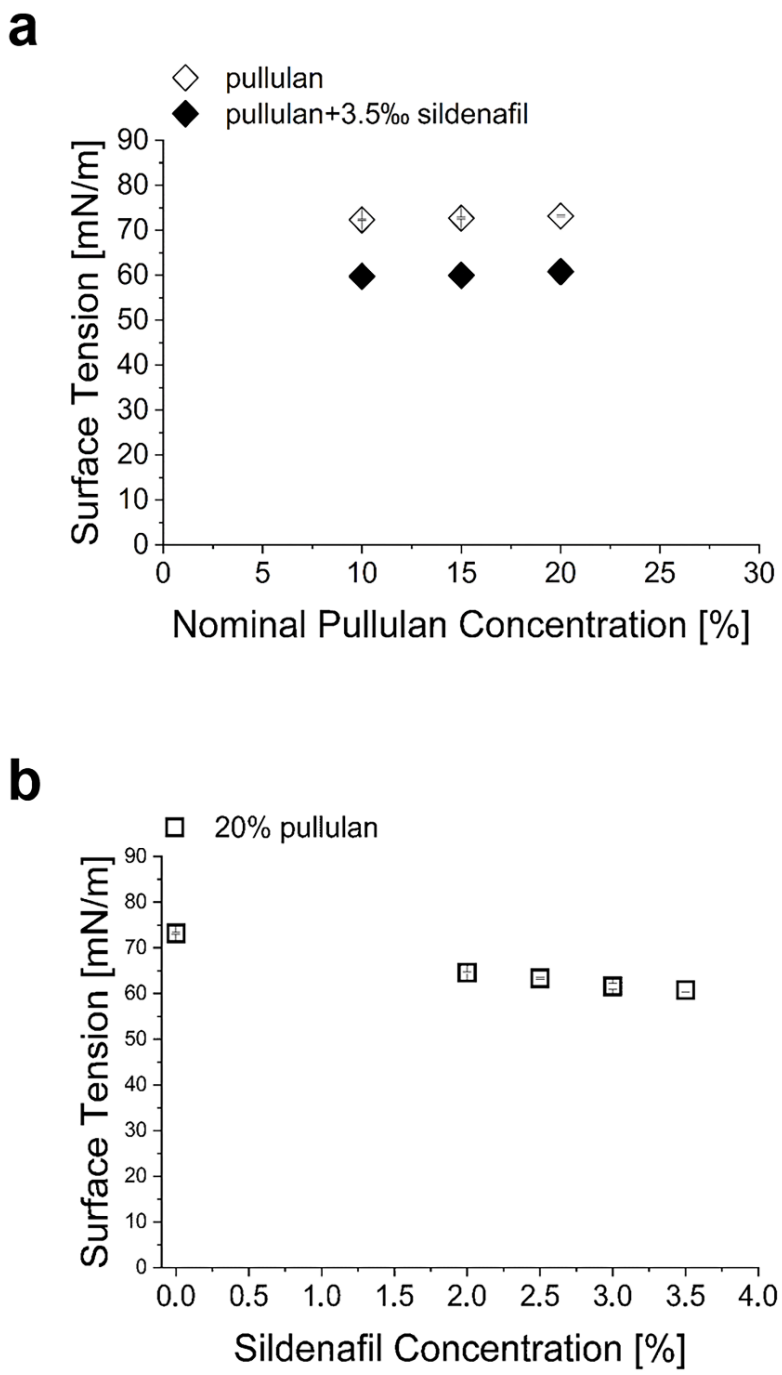

Figure 5: surface tension relevant to pullulan-based solutions containing either the polymer as such or with sildenafil. Effect of a) pullulan concentration and b) sildenafil content on a 20%wt pullulan-based solution.

Having as ultimate goal the manufacturing of non-woven structures to be used as ODFs, particular attention was paid to the electrospinning process. Besides attaining continuous, defect-free fibers with a diameter in the nanometer range, the need for getting a production rate as high as possible was also considered. In this respect, it is well-known that the use of viscous feedstock solutions has a beneficial

effect towards the formation of high-quality fibers, at least up to viscosity levels that hinder the flow of the solution through the spinning needle [Fong et al., 1999; Ramakrishna et al., 2005; Yang et al., 2004]. Moreover, the elastic component of the viscoelastic behavior of the starting formulation is recognized to play a preeminent role in determining both the feasibility of the electrospinning process and the attainment of fibers with uniform morphology [Formenti et al., 2016; Yu et al., 2006]. Finally, a solution having a relatively low surface tension would limit the extent of the Rayleigh instability, which is the main cause of the so-called "beads-on-strings". Based on those considerations and on the data collected so far, the formulation containing 20%wt of pullulan and saturated with sildenafil was deemed as the best compromise for the subsequent electrospinning studies. Moreover, it was expected to be characterized by a relatively faster solvent evaporation during processing and represented the best choice in view of obtaining the highest possible drug load.

3.2. Electrospinning

To contain the costs, the process was initially set-up using placebo solutions containing pullulan only, considering the production rate and the quality of the resulting fibers as the main outputs. Based on preliminary trials, aluminum foils were selected as collectors and horizontal spinning direction was preferred. Moreover, needle tip-to-collector-distance was set to 200 mm, in order to allow complete water evaporation and reduce the risk of sparks at the highest electric potential difference. On the other hand, flow rate and voltage were varied as reported in Table 1, in which the different background colors represent the overall quality of the fibers attained: green for defect-free fibers, yellow for acceptable fibers presenting minor defects and red for unsuitable defective fibers. By way of example, photographs of the collected non-woven mats taken at the optical microscope are reported within the Table.

Overall, high flow rate led to a decrease in product quality, which was counter-acted by increasing the potential difference. Typically, higher rates - and therefore greater amounts of polymeric formulations to be processed - require greater voltages to achieve a stable jet, as an increase stretching of the solution would be necessary. However, high voltages may cause instability of the jet, thus leading to the formation of fibers containing beads and with non-uniform diameter. In this respect, electrospinning conditions allowing to manufacture suitable placebo fibers at the highest production rate entailed a potential difference of 20kV and a solution flow rate of 5mL/hr.

Table 1: flow rate and voltage tested in electrospinning of the solution containing 20%wt of pullulan as such. Green, yellow and red colors are used to identify the quality of the fibers obtained. By way of example, some photographs representative of the fiber quality were also included.

V (mL/h) / ΔV (kV)	0.1	0.3	0.5	1	1.5	2	2.5	3	3.5	4	4.5	5	5.5	6
15														
16														
17														
18														
19														
20														
21														

Good	Few defects	Many defects
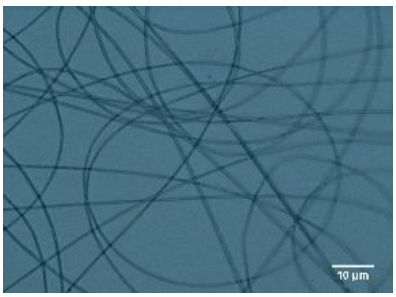	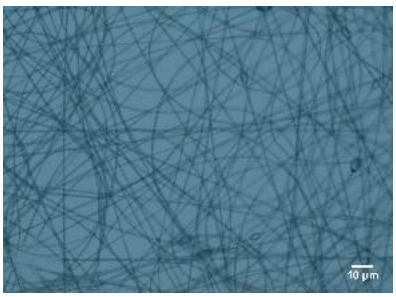	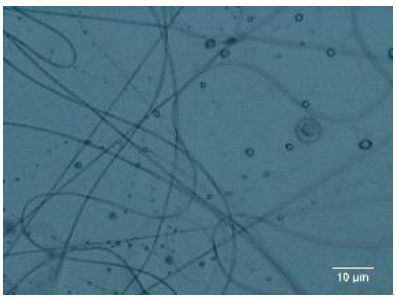

Moving to the sildenafil-containing formulation, the experimental field of investigation was reduced and limited to the operating parameters that previously led to fibers that were judged as either good or on average (*i.e.* green of yellow background in Table 1). Results of this second experimental phase of the work are summarized in Table 2.

Table 2: flow rate and voltage tested in electrospinning of the solution containing 20%wt of pullulan and sildenafil.

V (mL/h) / ΔV (kV)	0.1	0.3	0.5	1	1.5	2	2.5	3	3.5	4	4.5	5	5.5	6
15														
16														
17														
18														
19														
20														
21														

Interestingly, the maximum rate of production of fibers without defects was reduced from 5mL/h to 1-2mL/h. Given the very similar viscosity and relaxation time values found when testing placebo and drug-containing formulations and the lower surface tension of the solution containing sildenafil, an easier electrospinnability of the latter would have been expected. Therefore, an effect of sildenafil on the conductivity of pullulan solutions was hypothesized. This might have counterbalance the beneficial effect of the increase in potential difference and led to lower evaporation rate of feedstock formulations, as suggested by the occurrence of dripping phenomena and by the appearance of joined fibers (Supplementary material, Figure S2 and S3).

Both placebo and drug-containing solutions were electrospun in the conditions identified as suitable for the sildenafil-containing formulation, *i.e.* setting a flow rate of 1.0mL/h and a potential difference of 19-20kV, respectively. In Figure 6, SEM images of the fibers attained are reported. Overall, fiber diameter ranged from 400 nm to 700 nm in different samples, while within the same specimens the maximum variation observed was about 200 nm.

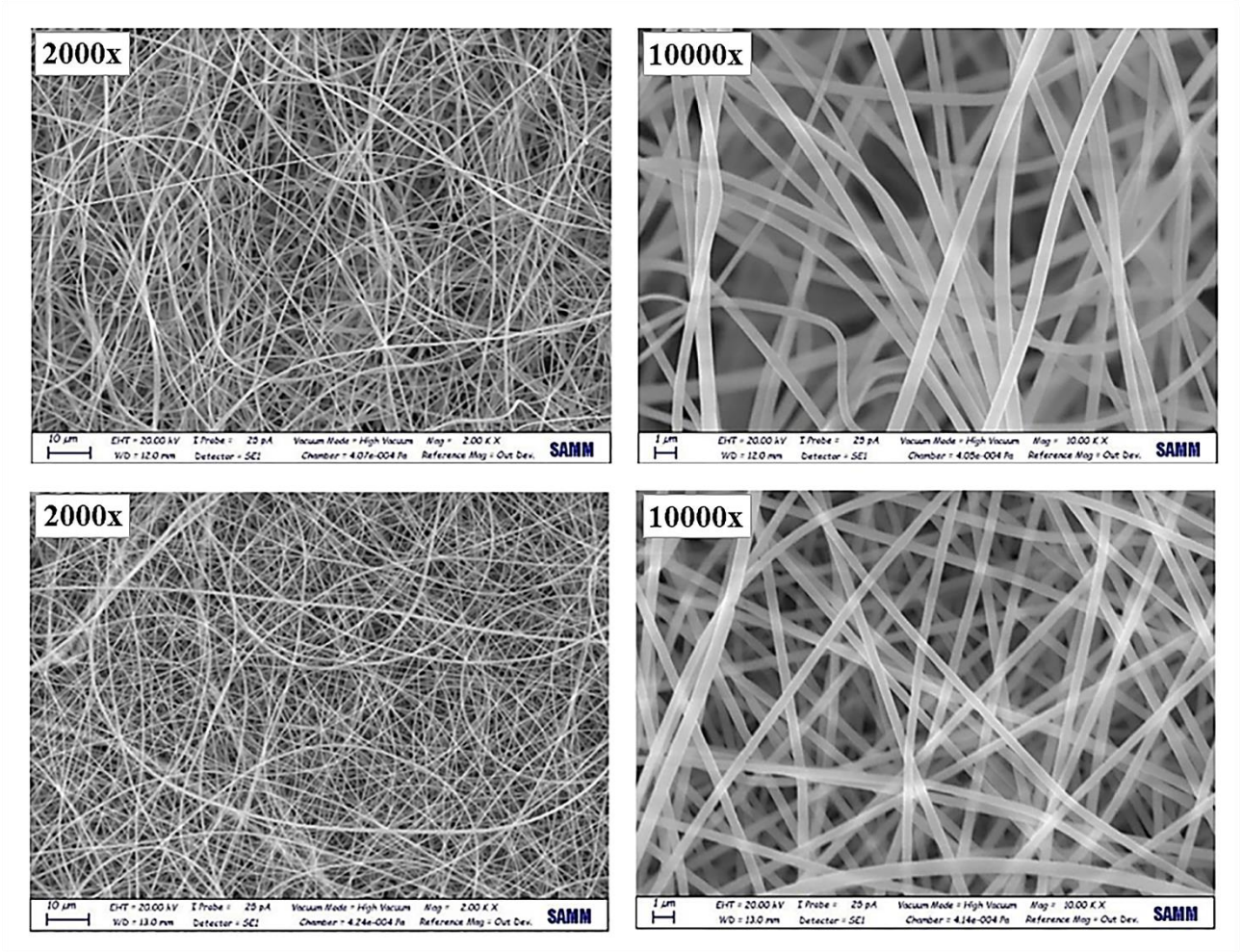

Figure 6: SEM photographs of electrospun films attained from solutions containing either (top) 20%wt of pullulan as such or (bottom) with sildenafil.

In order to evaluate the influence of the microstructure of the non-woven mat attained by electrospinning, films of analogous composition were also manufactured by either spin- or blade-coating, which were expected to led to continuous films with lower porosity. The IR spectra reported in Figure 7a, and in particular the position of the main peak of the structured band in the 1200 - 950 cm^{-1} region, revealed a more ordered morphology of pullulan in the non-woven-mat (blue line) with respect to the polymer powder (green line) and to samples obtained by spin-coating (orange line). Shingel and colleagues suggested that the bands at 1045 cm^{-1} and 1024 cm^{-1}, which are assigned to vibrational normal modes involving C-O stretching vibrations, could be related to chains belonging to crystalline and to amorphous phase of pullulan, respectively [Shingel et al., 2002]. On the other hand, because of the sensitivity of the vibrational frequencies to the molecular conformation, these bands could be considered as markers of chains characterized by either conformational order or showing a disordered molecular structure, independently of the formation of 3D crystalline domains.

This could explain why the 1045 cm^{-1} component resulted stronger in the IR spectrum relevant to electrospun pullulan fibers, if compared with the spin-coated film or with the polymer powder. Indeed, the electrospinning process is known to promote both polymeric chain alignment and elongated chains conformations, thus improving the conformational order of the molecular structure. The presence of sildenafil within the fibers was con-firmed by the small absorption feature arising at around 1700 cm^{-1}, as highlighted in Figure 7b. This shoulder corresponded to the strongest peak in the spectrum of sildenafil (violet line). However, no evidence of major pullulan-drug interaction has been detected. Given the very limited amount of sildenafil conveyed into the non-woven samples, no conclusions can be drawn about the presence of small crystallites versus isolated molecules of the drug after electrospinning.

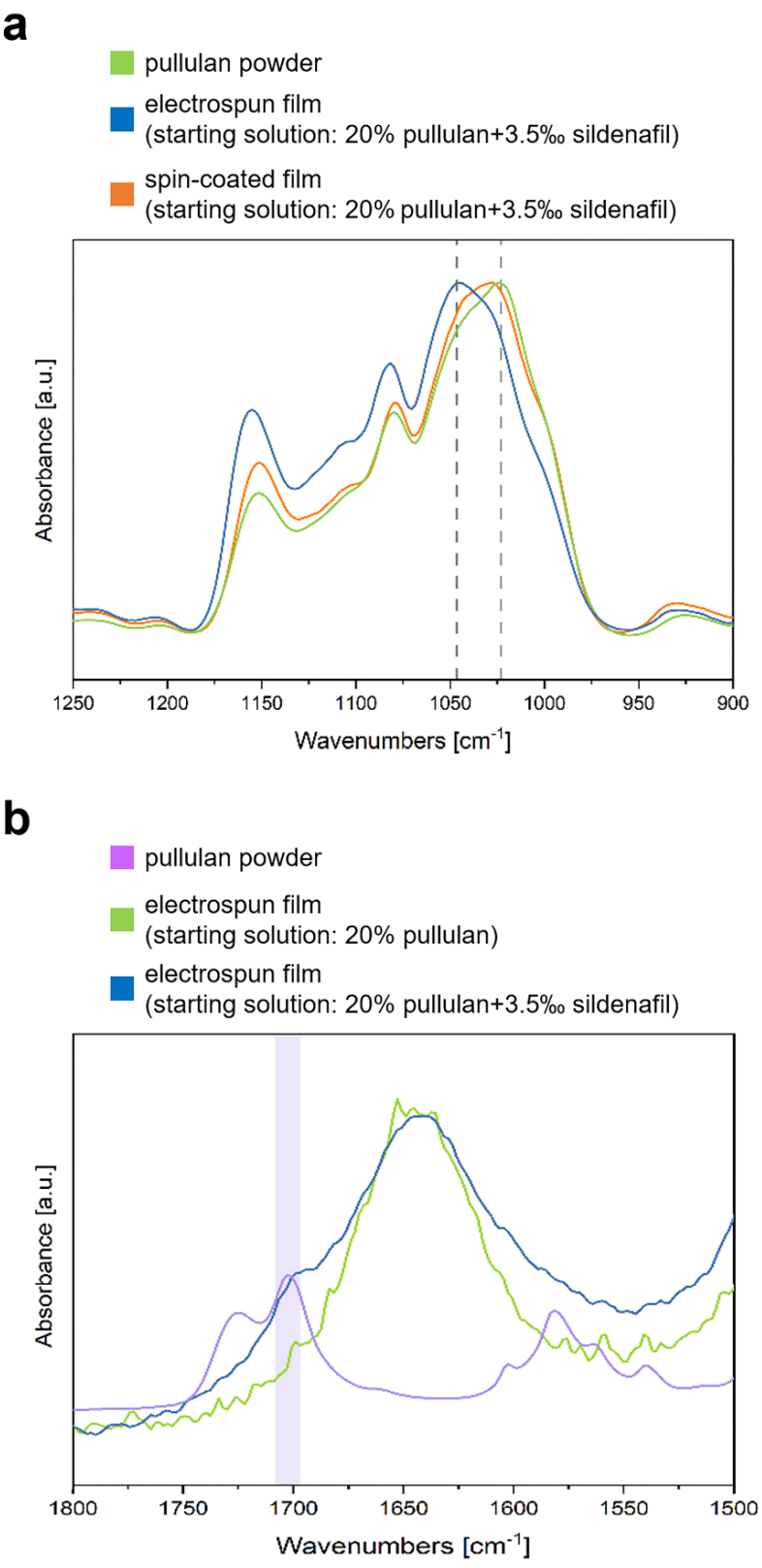

Figure 7: infrared spectra in the a) 1250 cm^{-1} - 900 cm^{-1} region and b) 1800 cm^{-1} - 1500 cm^{-1} region relevant to different samples.

The drug content in the electrospun films was found consistent with that of the starting solutions and with the nominal value. Indeed, data relevant to nominal 15mm x 15mm x 0.05mm ODFs samples, attained by cutting the non-woven mat, were: weight 5.35 mg (CV ≤ 5%), thickness 53 μm (CV ≤ 9%) and sildenafil content 76.498 μg (CV ≤ 5%). In this respect, the final drug load of approximately 70 μg might be compatible with the intended pediatric application, although relatively low. Moreover, the sildenafil content could be enhanced by increasing the dimensions of the film, especially its thickness, either by carrying out electrospinning for longer times or resorting to industrial level equipment with multiple spinnerets working in parallel. Electro-spinning pullulan-based solutions containing sildenafil in suspension could represent another interesting approach and trials are currently ongoing in this respect.

3.3. Interaction with aqueous fluids

The behavior of films upon contact with aqueous fluids was initially evaluated following Ph. Eur. and USP indications, thus considering 120 and 30 s as the cut-off values for disintegration. In order to rule out the possible impact of the electrospun product microstructure (*i.e.* presence of overlapping nano-fibers in a non-continuous mat) on ODFs performance, films having the same composition but manufactured by spin- and blade-coating were also considered for comparison purposes. Independent of the presence of sildenafil, these two type of films exceeded the compendial limits, with thicker samples needing more time to disintegrate (thickness ranged from 70.6 ± 9 μm to 95 ± 7.9 μm for blade-coated films and was about 10 μm for spin-coated ones). On the other hand, the performance of electrospun products turned out always acceptable. In order to deepen the behavior of the latter upon contact with aqueous fluids, a purposely-developed method, set up as described in the Material and Methods sections, was adopted, during which the disintegration time was visually evaluated and identified as the time needed for the film to disappear (Table 3).

Table 3: disintegration times relevant to different electrospun films (maximum recording time was 6s).

	Film thickness, µm	Disintegration time, s
Placebo films	45	>6*
	50	>6*
	55	>6*
	230**	>6*
	200**	>6*
Sildenafil-containing films	40	6
	50	6
	51	4.2
	58	4.2
	74	2.8
	80**	4.8
	158**	>6*

* The sample did not disintegrate/dissolve completely during the recording

** Data relevant to overlapped films

Placebo electrospun films immediately (within 0.2 s) started to shrink upon con-tact with the medium, being completely wet and transparent in less than 0.5 s. By adding the extra liquid (2 mL), the samples broke up further, but they did not seem to completely disintegrate/dissolve within the time frame considered, although after approximately 5 s they resulted practically invisible. However, using a glass stirrer into the petri dish, the presence of film residues could still be detected. By way of example, photographs of an electrospun placebo film tested in the dedicated setup are reported in Figure 8 (full sequence is available in Supplementary material, Video S4).

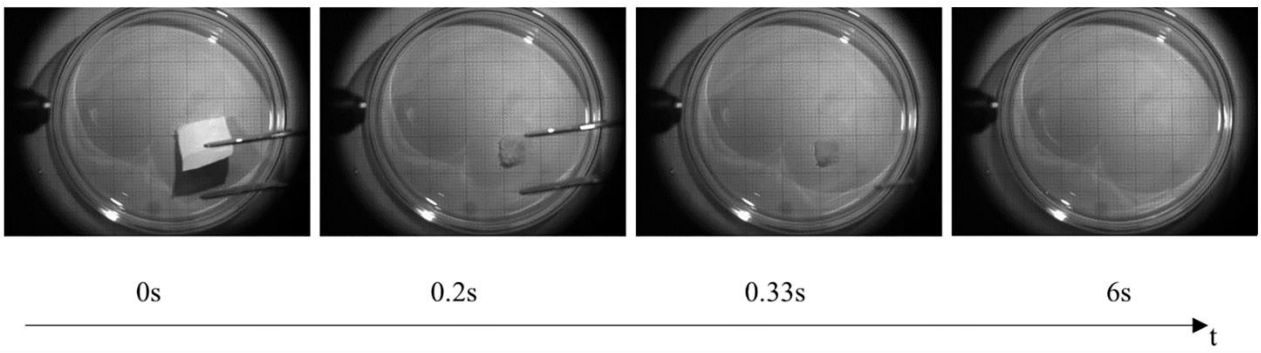

Figure 8: photographs of an electrospun placebo film (45 µm thick) upon contact with water.

Conversely, electrospun products containing 3.5‰wt of sildenafil were characterized by a sort of blow up behavior immediately upon contact with the aqueous me-dia. They seemed to explode in many small fragments so as, even before the addition of the extra 2 mL of water, no residues were easily visible (< 3s). By way of example, Figure 9 reports the performance of a drug-containing electrospun sample (full sequence in Supplementary material, Video S5).

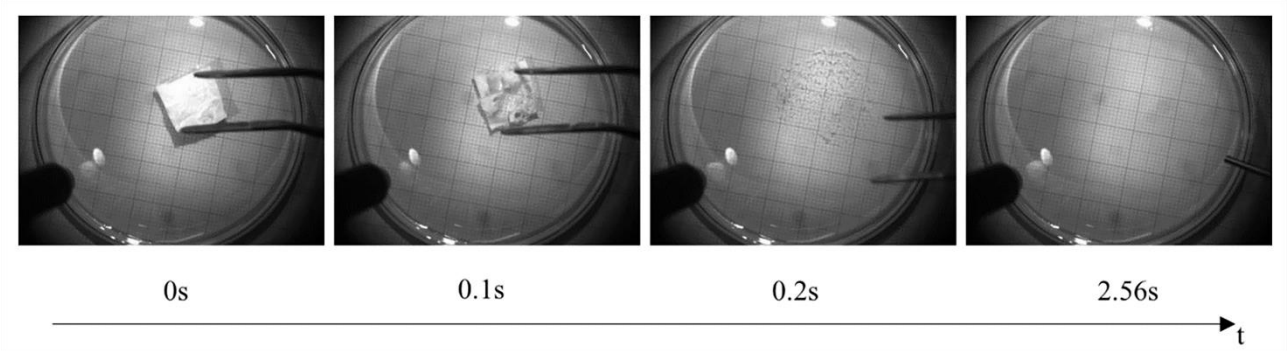

Figure 9: photographs of an electrospun sildenafil-containing film (74 µm thick) upon contact with water.

Based on the data collected with non-woven products, placebo-pullulan films mainly underwent a dissolution process, which was relatively slow, as already reported by Chachlioutaki and co-workers [Chachlioutaki et al., 2020]. When dealing with sildenafil-containing samples, the active ingredient immediately dissolved upon contact with water, probably thanks to the very high surface-to-volume ratio electrospun specimens are provided with. Due to this rapid drug solubilization, the continuity of the fibers in the non-woven mat was lost. At the same time, pullulan started swelling (with possible release of stresses internal to the fibers), thus leading to the above-mentioned blow up effect. As a consequence, the fiber fragments were pushed apart one from the other with the resulting small debris start dissolving, which occurred quite fast in view of their limited dimensions. The experiments were repeated several times, on drug-containing and placebo samples having different thickness and belonging to di-verse electrospinning batches, but the peculiar behavior above described was always highlighted. Further work would be required to better characterize such films, for in-stance to deepen possible changes in the conductivity/nanostructure of the electrospun samples from sildenafil-containing solutions.

4. Conclusion

ODFs, which are devised to disintegrate/dissolve almost instantaneously in the saliva without water, are recognized as a patient-centric dosage form with high compliance, especially in patients having swallowing limitations. To the best of our knowledge, this is the first work evaluating the feasibility of electrospinning, starting from pullulan-based aqueous solutions, in the manufacturing of ODFs intended for fast release of sildenafil to pediatric patients with persistent pulmonary hypertension. This application was deemed particularly interesting as promising data on bioavailability improvement of sildenafil, following relevant formulation in ODFs, have recently been collected in healthy men [De Toni et al., 2018; Loprete et al., 2018]. The possibility to resort to simple solutions (*i.e.* using water as the only solvent and containing just natural pullulan as well as the active ingredient) for the continuous production of good quality fibers with uniform diameter in the nanometer range was demonstrated, being the final ODFs characterized by high potential towards patient safety. The use of pullulan turned out promising not only from a manufacturing standpoint, in terms of process times and relevant robustness, but also in view of the very low disintegration time the resulting ODFs were provided with. Unfortunately, the sildenafil load into the nanofibers was limited by the drug solubility. However, this issue might be overcome by resorting to industrial-scale equipment, that generally couple multiple spinnerets working in parallel. Moreover, the drug content be also improved by increasing drug solubility, *e.g.* by working at high temperatures or making use of co-solvents [Torres-Martínez et al., 2020]. Although the latter option would have the further advantage to increase the solvent evaporation rate, the former one would be preferable in view of the final pharmaceutical applications of the resulting electro-spun products. Another possible approach might be represented by the idea of electrospinning a sildenafil suspension. Taking into account all the above-mentioned possibilities, some promising preliminary experiments are currently ongoing.

Supplementary Material

Figure S1: zero shear viscosity of solutions containing 20%wt of pullulan and increasing amounts of sildenafil (2‰wt, 2.5‰wt, 3‰wt, 3.5‰wt).

Figure S2: photograph taken at the optical microscope (5x magnification) highlighting the effect of dripping during ele-trospinning of the solution containing 20%wt of pullulan and 3.5‰wt of sildenafil (operating conditions: 16kV, 4.0mL/h, 200mm TCD, 22.4°C and RH 27%).

Figure S3: SEM photographs highlighting the effect of residual water content (possibly combined with electrostatic effect) during electrospinning of the solution containing 20%wt of pullulan and saturated with sildenafil (operating conditions: 20kV, 1.0mL/h, 200mm TCD, 21.7°C and RH 32%).

All data supporting reported results are available upon request to the corresponding authors.

Acknowledgments

The authors wish to thank Mr. Takanobu Higashiyama from HAYASHI-BARA CO., LTD for supplying the pullulan material and for the fruitful discussions and Prof. Chiara Castiglioni from Politecnico di Milano for the support in the interpretation of FT-IR results.

Conflicts of Interest

The authors declare no conflict of interest.

References

Abman S.H., Hansmann G., Archer S.L., Ivy D.D., Adatia I., Chung W.K., Hanna B.D., Rosenzweig E.B., Raj J.U., Cornfield D., Stenmark K.R., Steinhorn R., Thébaud B., Fineman J.R., Kuehne T., Feinstein J.A., Friedberg M.K., Earing M., Barst R.J., Keller R.L., Kinsella J.P., Mullen M., Deterding R., Kulik T., Mallory G., Humpl T., Wessel D.L., Pediatric Pediatric pulmonary hypertension: guidelines from the American heart association and American thoracic society, Circulation, 2015, 132 :2037-2099

Andreadis I.I., Gioumouxouzis C.I., Eleftheriadis G.K., Fatouros D.G., The advent of a new era in digital healthcare: a role for 3D printing technologies in drug manufacturing?, Pharmaceutics, 2022, 14: 609

Anna S. L., McKinley G.H., Elasto-capillary thinning and breakup of model elastic liquids, Rheol., 2001, 45: 115-138

Badhwar P., Dubey K.K., Insights of microbial pullulan production: a bioprocess engineer assessment, Curr. Biotechnol., 2018, 7:262-272

Balusamy B., Celebioglu A., Senthamizhan A., Uyar T., Progress in the design and development of “fast-dissolving” electrospun nanofibers based drug delivery systems - A systematic review, J. Control. Release, 2020, 326: 482-509

Chachlioutaki K., Tzimtzimis E.K., Tzetzis D., Chang M.-W., Ahmad Z., Karavasili C., Fatouros D.G., Electrospun orodispersible films of isoniazid for pediatric tuberculosis treatment, Pharmaceutics, 2020, 12: 470

Cleeton C., Keirouz A., Chen X., Radacsi N., Electrospun nanofibers for drug delivery and biosensing, ACS Biomater. Sci. Eng., 2019, 5: 4183-4205

De Toni L., Ponce M.R., Franceschinis E., Dall'Acqua S., Padrini R., Realdon N., Garolla A., Foresta C., Sublingual administration of sildenafil orodispersible film: New profiles of drug tolerability and pharmacokinetics for PDE5 inhibitors, Front. Pharmacol., 2018, 9: 59

Dhariwal A.K., Bavdekar S.B., Sildenafil in pediatric pulmonary arterial hypertension, J. Postgrad. Med., 2015, 61: 181-192

Doostmohammadi M., Forootanfar H., Ramakrishna S., Regenerative medicine and drug delivery: Progress via electrospun biomaterials, Mater. Sci. Eng. C, 2020, 109: 110521

Entov V.M., Hinch, E.J., Effect of a spectrum of relaxation times on the capillary thinning of a filament of elastic liquid, J. Nonnewton. Fluid. Mech., 1997, 72: 31-53

Evers P.D., Critser P.J., Cash M., Magness M., Hoelle S., Hirsch R., Cost-utility of sildenafil for persistent pulmonary hypertension of the newborn, Am. J. Perinatol., 2021, 38: 1505-1512

Ferlak J., Guzenda W., Osmałek T., Orodispersible films - Current state of the art, limitations, Advances and future perspectives, Pharmaceutics, 2023, 15 :361

Fong H., Chun I., Reneker D., Beaded nanofibers formed during electrospinning. Polymer, 1999, 40: 4585–4592

Formenti S., Castagna R., Momentè R., Bertarelli C., Briatico-Vangosa F., The relevance of extensional rheology on electro-spinning: the polyamide/iron chloride case, Eur. Polym. J., 2016, 75:46-55.

Gao X., Han S., Zhang R., Liu G., Wu J., Progress in electrospun composite nanofibers: composition, performance and applications for tissue engineering, J. Mater. Chem. B, 2019,7: 7075-7089

Garsuch V., Breitkreutz J., Comparative investigations on different polymers for the preparation of fast-dissolving oral films, J. Pharm. Pharmacol., 2010, 62: 539-545

George A., Shah P.A., Shrivastav P.S., Natural biodegradable polymers based nano-formulations for drug delivery: a review, Int. J. Pharm., 2019, 561: 244-264

Guo Y., Wang X., Shen Y., Research progress, models and simulation of electrospinning technology: a review, J. Mater. Sci., 2022, 57: 58-104

Gupta M.S., Kumar T.P., Davidson R., Kuppu G.R., Pathak K., Gowda D.V., Printing methods in the production of orodispersible films, AAPS PharmSciTech., 2021, 22: 129

Hassan M. Ibrahim, Anke Klingner, A review on electrospun polymeric nanofibers: production parameters and potential applications, Polym. Test., 2020, 90: 106647

He M., Zhu L., Yang N., Li H., Yang Q., Recent advances of oral film as platform for drug delivery, Int. J. Pharm., 2021a, 604: 120759

He Z., Zhu S., Zhou K., Jin Y., He L., Xu W., Lao C., Liu G., Han S., Sildenafil for pulmonary hypertension in neonates: An updated systematic review and meta-analysis, Pediatr. Pulmonol. 2021b, 56: 2399-2412

Hoffmann E.M., Breitenbach A., Breitkreutz J., Advances in orodispersible films for drug delivery, Expert Opin. Drug Deliv., 2011, 8: 299-316

Ignatious F., Sun L., Lee C.-P., Baldoni J., Electrospun nanofibers in oral drug delivery, Pharm. Res., 2010, 27: 576-588

Ignatova M., Rashkov I., Manolova N., Drug-loaded electrospun materials in wound-dressing applications and in local cancer treatment, Expert Opin. Drug Deliv., 2013, 10: 469-483

Kallakunta V.R., Sarabu S., Bandari S., Tiwari R., Patil H., Repka M.A., An update on the contribution of hot-melt extrusion technology to novel drug delivery in the twenty-first century: part I, Expert Opin. on Drug Deliv., 2019, 16: 539-550

Kean E.A., Adeleke O.A., Orally disintegrating drug carriers for paediatric pharmacotherapy, Eur. J. Pharm. Sci., 2023: 182: 106377

Khalid G.M., Musazzi U.M., Selmin F., Franzè S., Minghetti P., Cilurzo F., Extemporaneous printing of diclofenac orodispersible films for pediatrics, Drug Dev. Ind. Pharm., 2021a, 47: 636-644,

Khalid G.M., Selmin F., Musazzi U.M., Gennari C.G.M., Minghetti P., Cilurzo F., Trends in the characterization methods of orodispersible films, Curr. Drug Deliv., 2021b, 18: 935-946

Kumar, L., Verma, S., Joshi, K., Utreja P., Sharma S., Nanofiber as a novel vehicle for transdermal delivery of therapeutic agents: challenges and opportunities, Futur. J. Pharm, Sci., 2021, 7: 175

Laudenslager M.J., Sigmund W.M., Electrospinning. In: Bhushan, B. (eds) Encyclopedia of Nanotechnology. Springer, Dordrecht, The Netherlands, 2012.

Leathers T.D., Biotechnological production and applications of pullulan, Appl. Microbiol. Biotechnol., 2003, 62:468-473

Li Z., Lv X., Liu Q., Dang D., Wu H., Update on the use of sildenafil in neonatal pulmonary hypertension: a narrative review of the history, current administration, and future directions, Transl. Pediatr., 2021, 10: 998-1007

Loprete L., Leuratti C., Frangione V., Radicioni M., Pharmacokinetics of a novel sildenafil orodispersible film administered by the supralingual and the sublingual route to healthy men, Clin. Drug Investig., 2018, 38: 765-772

Luraghi A., Peri F., Moroni L., Electrospinning for drug delivery applications: a review, J. Control. Release, 2021, 334: 463-484

Madruga L.Y.C., Kipper M.J., Expanding the repertoire of electrospinning: new and emerging biopolymers, techniques, and applications, Adv. Healthc. Mater., 2022, 11: 2101979

McKinley G.H., Sridhar T., Filament-stretching rheometry of complex fluids, Ann. Rev. Fluid Mech., 2002, 34: 375-415

Meinel A.J., Germershaus O., Luhmann T., Merkle H.P., Meinel L., Electrospun matrices for localized drug delivery: Current technologies and selected biomedical applications, Eur. J. Pharm. Biopharm., 2012, 81: 1-13

Melocchi A., Uboldi M., Cerea M., Foppoli A., Maroni A., Moutaharrik S., Palugan L., Zema L., Gazzaniga A., Shape memory materials and 4D printing in pharmaceutics, Adv. Drug Deliv. Rev., 2021,173: 216-237

Musazzi U.M., Khalid G.M., Selmin F., Minghetti P., Cilurzo F., Trends in the production methods of orodispersible films, Int. J. of Pharm., 2020, 576: 118963

Ngwuluka N.C., Ochekpe N.A., Aruoma O.I., Naturapolyceutics: The science of utilizing natural polymers for drug delivery, Polymers, 2014, 6: 1312-1332

Nichols D.J., Muirhead G.J., Harness J.A., Pharmacokinetics of sildenafil after single oral doses in healthy male subjects: absolute bioavailability, food effects and dose proportionality, Br. J. Clin. Pharmacol., 2002, 53:5S-12S

Ouranidis A., Tsiaxerli A., Vardaka E., Markopoulou C.K., Zacharis C.K., Nicolaou I., Hatzichristou D., Haidich A.B., Kostomitsopoulos N., Kachrimanis K., Sildenafil 4.0-Integrated synthetic chemistry, formulation and analytical strategies effecting immense therapeutic and societal impact in the fourth industrial era, Pharmaceuticals, 2021, 14: 365.

Persano, L.; Camposeo, A.; Tekmen, C.; Pisignano, D. Industrial Upscaling of Electrospinning and Applications of Polymer Nanofibers: A Review, Macr. Mat. and Eng., 2013, 298:504

Ponrasu T., Chen B.H., Chou T.H., Wu J.J., Cheng Y.S., Fast dissolving electrospun nanofibers fabricated from jelly fig poly-saccharide/pullulan for drug delivery applications, Polymers, 2021, 13:241

Preis M., Woertz C., Kleinebudde P., Breitkreutz J., Oromucosal film preparations: Classification and characterization methods, Expert Opin. Drug Deliv., 2013, 10: 1303-1317

Qi Z., Yu H., Chen Y., Zhu M., Highly porous fibers prepared by electrospinning a ternary system of nonsolvent/solvent/poly(l-lactic acid), Mater. Lett., 2009, 63: 415-418

Qin Z.-Y., Jia X.-W., Liu Q., Kong B.-H., Wang H., Fast dissolving oral films for drug delivery prepared from chitosan/pullulan electrospinning nanofibers, Int. J. Biol. Macromol., 2019, 137: 224-231

Ramakrishna S., Fujihara K., Teo W.E., Lim T.C., Ma Z., An introduction to electrospinning and nanofibers, World Scientific Publishing Co., London, UK, 2005.

Saab M., Mehanna M.M., Disintegration time of orally dissolving films: various methodologies and in-vitro/in-vivo correlation, Pharmazie, 2019, 74: 227-230

Sarabu S., Bandari S., Kallakunta V.R., Tiwari R., Patil H., Repka M.A., An update on the contribution of hot-melt extrusion technology to novel drug delivery in the twenty-first century: part II, Expert Opin. Drug Deliv., 2019, 16: 567-582

Scarpa M., Stegemann S., Hsiao W.-K., Pichler H., Gaisford S., Bresciani M., Paudel A., Orlu M., Orodispersible films: Towards drug delivery in special populations, Int. J. Pharm., 2017, 523: 327-335

Shingel K.I., Determination of structural peculiarities of dexran, pullulan and gamma-irradiated pullulan by Fourier-transform IR spectroscopy, Carbohydr. Res., 2002, 337: 1445-1451

Si Y., Shi S., Hu J., Applications of electrospinning in human health: from detection, protection, regulation to reconstruction, Nano Today, 2023, 48: 101723

Singh R.S., Kaur N., Rana V., Kennedy J.F., Pullulan: A novel molecule for biomedical applications, Carbohydr. Polym., 2017, 171: 102-121

Slavkova M., Breitkreutz J., Orodispersible drug formulations for children and elderly, Eur. J. Pharm. Sci., 2015, 75: 2-9

Sun X.B., Jia D., Kang W.M., Cheng B.W., Li Y.B., Research on electrospinning process of pullulan nanofibers, Appl. Mech. Mater., 2012, 268-270, 198-201.

Torres-Martínez E.J., Vera-Graziano R., Cervantes-Uc J.M., Bogdanchikova N., Olivas-Sarabia A., Valdez-Castro R., Serra-no-Medina A., Iglesias A.L., Pérez-González G.L., Cornejo-Bravo J.M., Preparation and characterization of electrospun fibrous scaffolds of either PVA or PVP for fast release of sildenafil citrate, e-Polymers, 2020, 20: 746-758

Verbeke K., Formenti S., Vangosa F.B., Mitrias C., Reddy N.K., Anderson P D., Clasen, C., Liquid bridge length scale based nondimensional groups for mapping transitions between regimes in capillary break-up experiments, Phys. Rev. Fluids, 2020, 5: 051901

Visser J.C., Woerdenbag H.J., Hanff L.M., Frijlink H.W., Personalized Medicine in pediatrics: the clinical potential of orodispersible films, AAPS PharmSciTech., 2017, 18: 267-272

Xu X., Lv H., Zhang M., Wang M., Zhou Y., Liu Y., Yu D.-G., 2023, Recent progress in electrospun nanofibers and their applications in heavy metal wastewater treatment, Front. Chem. Sci. Eng., 2023, 16, 249-275

Yang Q., Li Z., Hong Y., Zhao Y., Qiu S., Wang C., Wei Y., Influence of solvents on the formation of ultrathin uniform poly(vinyl pyrrolidone) nanofibers with electrospinning, J. Polym. Sci. B Polym. Phys., 2004, 42: 3721-3726

Yu J.H., Fridrikh S.V., Rutledge G.C., The role of elasticity in the formation of electrospun fibers, Polymer, 2006, 47: 4789-4797

Zema L., Loreti G., Melocchi A., Maroni A., Gazzaniga A., Injection Molding and its application to drug delivery, J. Control. Release, 2012, 159: 324-331

Zema L., Melocchi A., Maroni A., Gazzaniga A., Three-dimensional printing of medicinal products and the challenge of personalized therapy, J. Pharm. Sci., 2017, 106: 1697-1705

Zhan L., Deng J., Ke Q., Li X., Huang C., Liu X., Qian L., Grooved fibers: preparation principles through electrospinning and potential applications, Adv. Fiber Mater., 2022, 4: 203-213

Zhang Q., Xu B., Lv J., Wang Z., Du J., Safety and effect of sildenafil on treating paediatric pulmonary arterial hypertension: A meta-analysis on the randomised controlled trials, Cardiol. Young, 2020, 30: 1882-1889

Declaration of interests

☒ The authors declare that they have no known competing financial interests or personal relationships that could have appeared to influence the work reported in this paper.

☐The authors declare the following financial interests/personal relationships which may be considered as potential competing interests:

Elisabetta Ravasi (E.R.), Alice Melocchi (A.M.), Alessia Arrigoni (A.A.), Arianna Chiappa (A.C.), Chiara Grazia Milena Gennari (C.G.), Marco Uboldi (M.U.), Chiara Bertarelli (C.B.), Lucia Zema (L.Z.) and Francesco Briatico Vangosa (F.B.V).

Conceptualization: F.B.V. and A.M.
Methodology: F.B.V., A.M. and C.B, C.G.
Investigation: E.R., A.A., C.G., A.C.
Data curation: E.R. F.B.V.
Writing-original draft preparation: F.B.V.
Writing-review and editing: L.Z, A.M., M.U.
Supervision: L.Z.
Resources: F.B.V, L.Z, C.B.

Figure 1

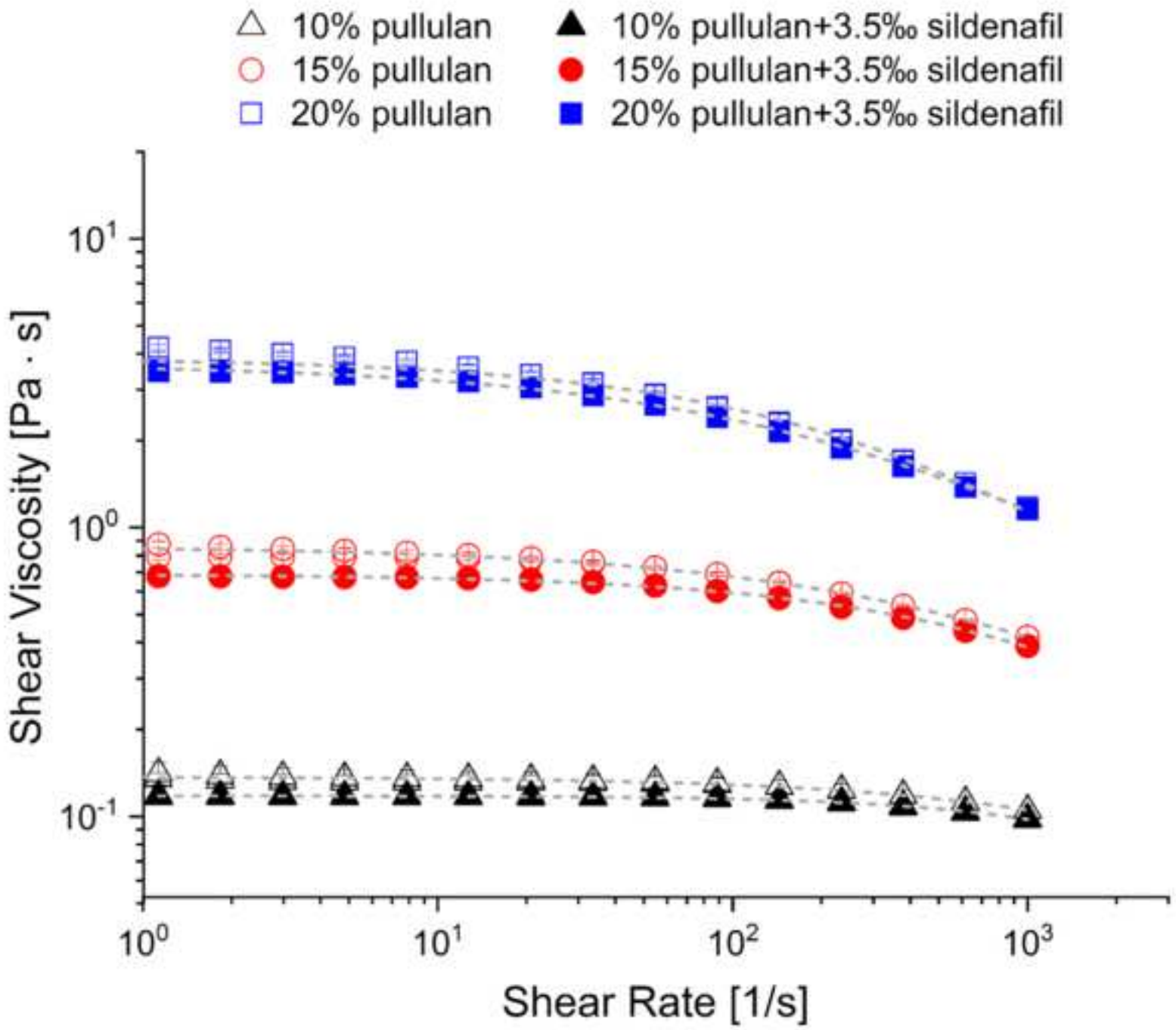
10% pullulan
15% pullulan
20% pullulan
10% pullulan+3.5‰ sildenafil
15% pullulan+3.5‰ sildenafil
20% pullulan+3.5‰ sildenafil
Shear Viscosity [Pa · s]
10^1
10^0
10^-1
10^0
10^1
10^2
10^3
Shear Rate [1/s]

Figure 2

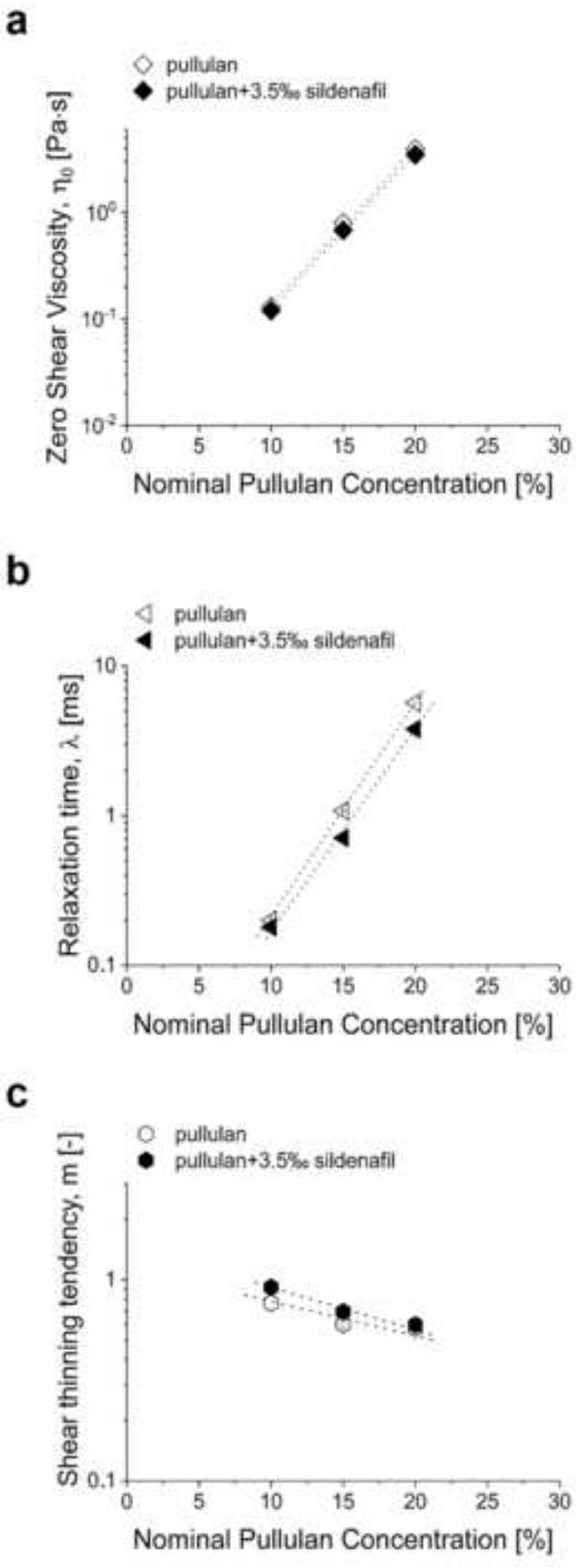
a
pullulan
pullulan+3.5‰ sildenafil
Zero Shear Viscosity, η_0 [Pa·s]
10^0
10^{-1}
10^{-2}
0
5
10
15
20
25
30
Nominal Pullulan Concentration [%]
b
pullulan
pullulan+3.5‰ sildenafil
Relaxation time, λ [ms]
10
1
0.1
0
5
10
15
20
25
30
Nominal Pullulan Concentration [%]
c
pullulan
pullulan+3.5‰ sildenafil
Shear thinning tendency, m [-]
1
0.1
0
5
10
15
20
25
30
Nominal Pullulan Concentration [%]

Figure 3

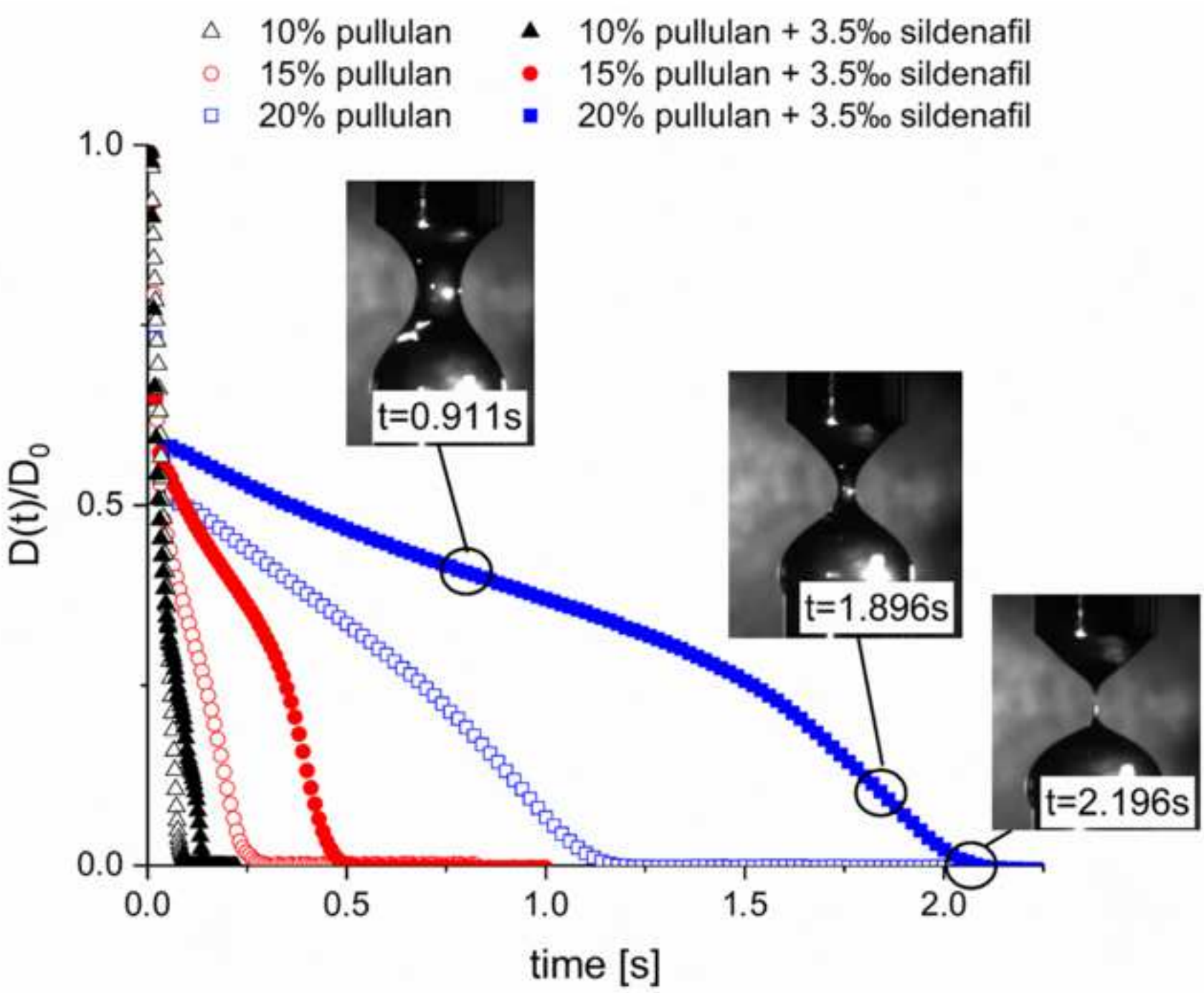
10% pullulan
15% pullulan
20% pullulan
10% pullulan + 3.5‰ sildenafil
15% pullulan + 3.5‰ sildenafil
20% pullulan + 3.5‰ sildenafil
D(t)/D0
1.0
0.5
0.0
0.0
0.5
1.0
1.5
2.0
time [s]
t=0.911s
t=1.896s
t=2.196s

Figure 4

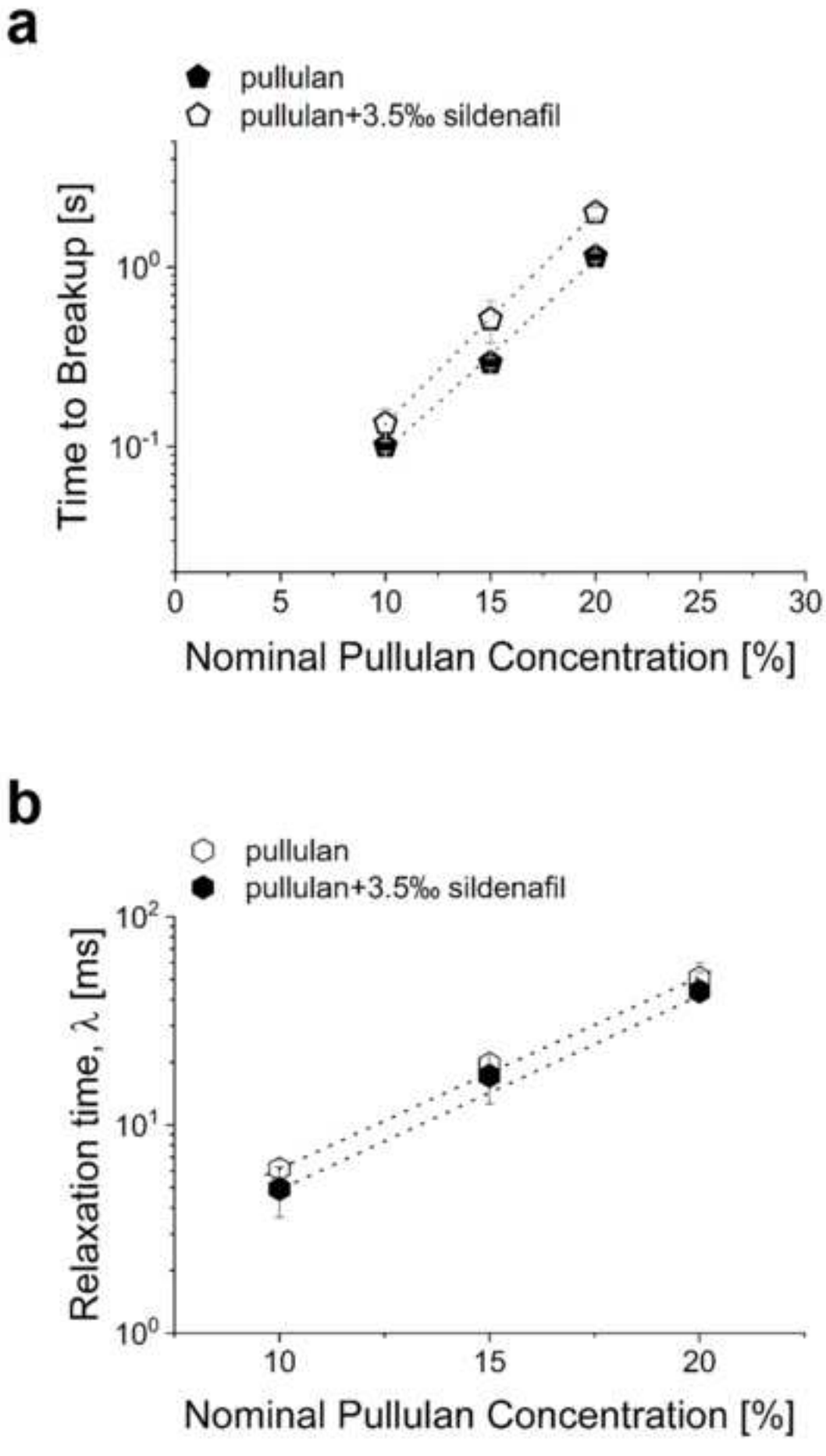
a
pullulan
pullulan+3.5‰ sildenafil
Time to Breakup [s]
10^0
10^{-1}
0
5
10
15
20
25
30
Nominal Pullulan Concentration [%]
b
pullulan
pullulan+3.5‰ sildenafil
Relaxation time, λ [ms]
10^2
10^1
10^0
10
15
20
Nominal Pullulan Concentration [%]

Figure 5

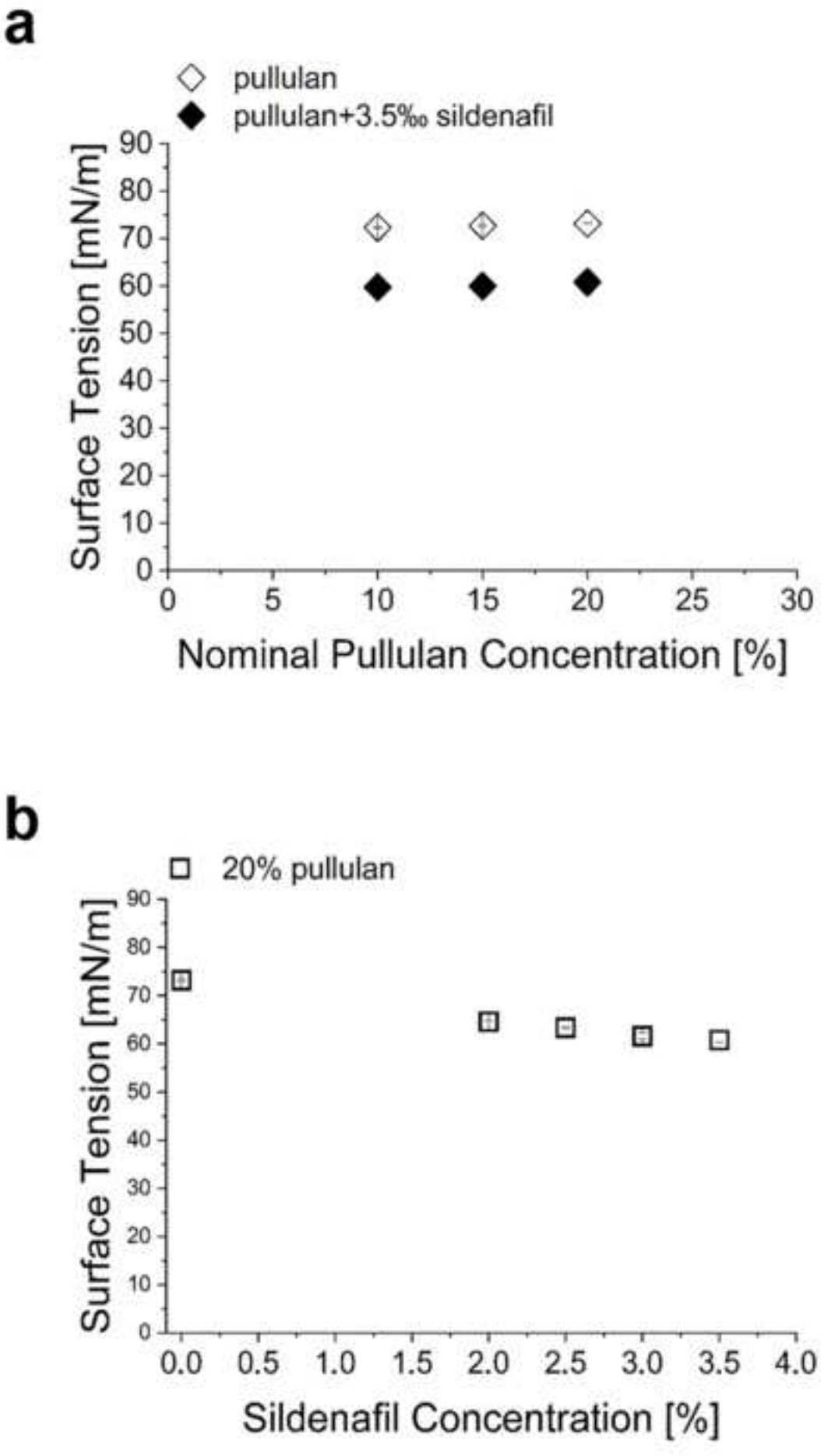
a
pullulan
pullulan+3.5‰ sildenafil
Surface Tension [mN/m]
0
10
20
30
40
50
60
70
80
90
0
5
10
15
20
25
30
Nominal Pullulan Concentration [%]
b
20% pullulan
Surface Tension [mN/m]
0
10
20
30
40
50
60
70
80
90
0.0
0.5
1.0
1.5
2.0
2.5
3.0
3.5
4.0
Sildenafil Concentration [%]

Figure 6

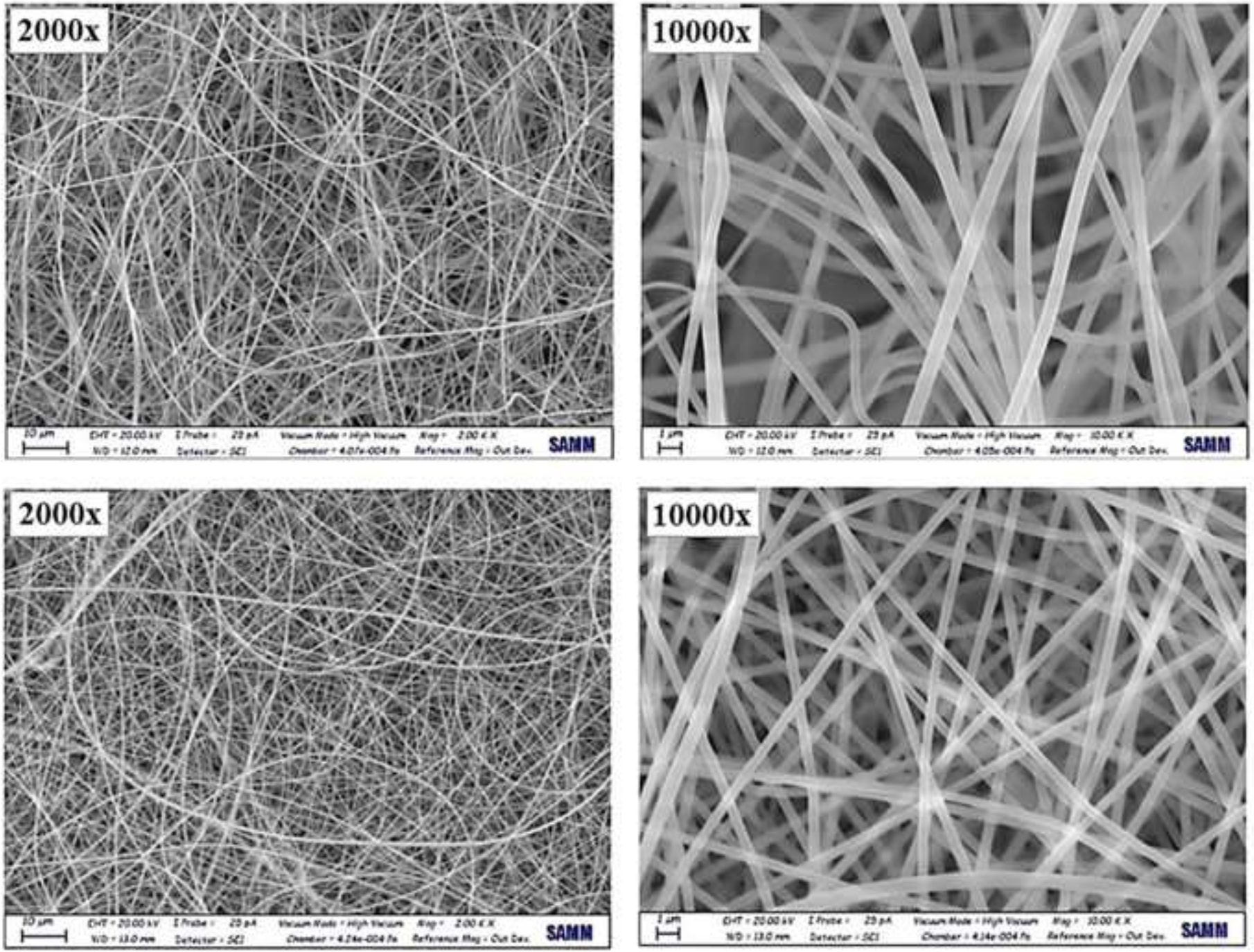

Figure 7

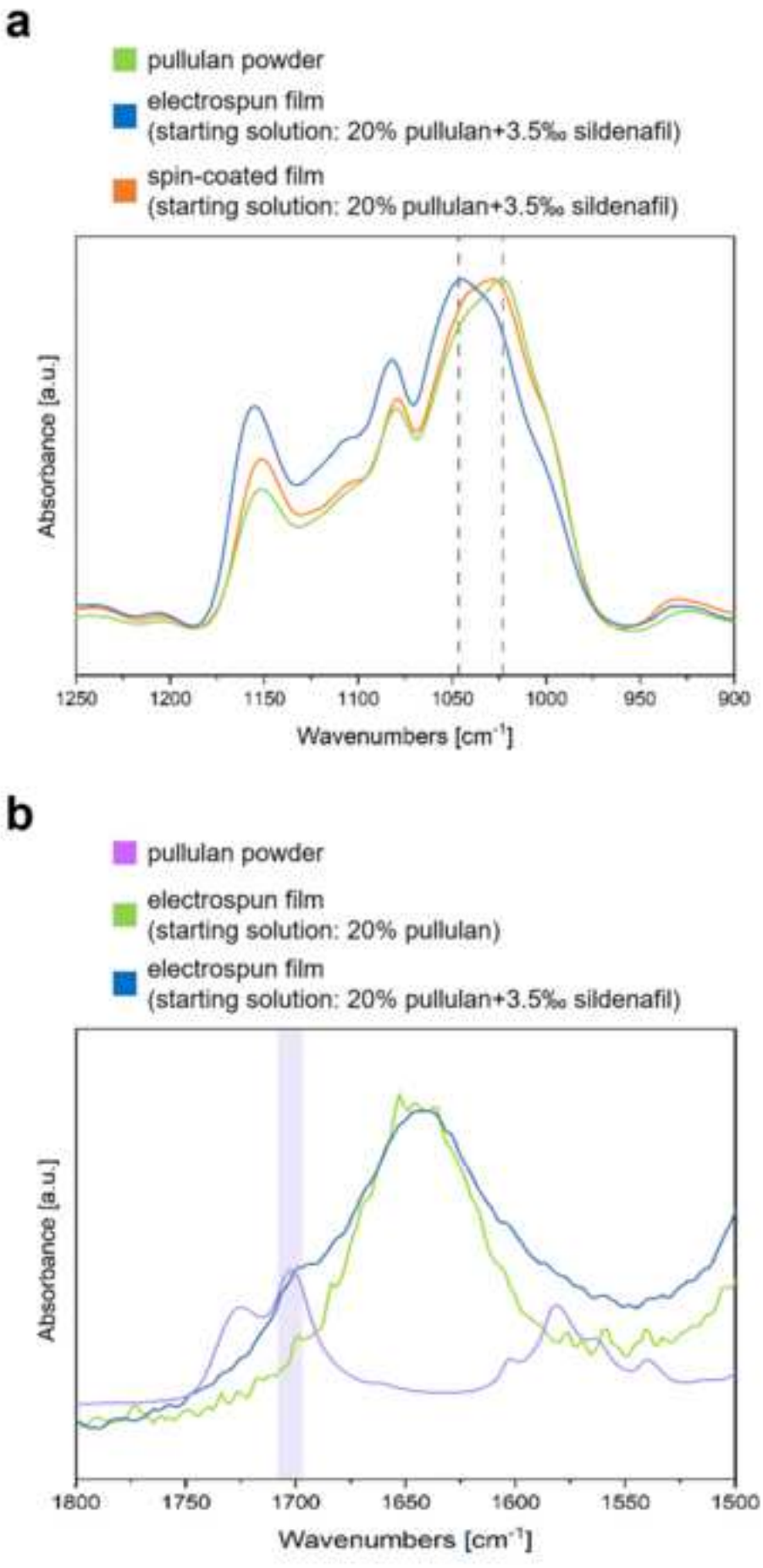
a
pullulan powder
electrospun film
(starting solution: 20% pullulan+3.5‰ sildenafil)
spin-coated film
(starting solution: 20% pullulan+3.5‰ sildenafil)
Absorbance [a.u.]
1250
1200
1150
1100
1050
1000
950
900
Wavenumbers [cm-1]
b
pullulan powder
electrospun film
(starting solution: 20% pullulan)
electrospun film
(starting solution: 20% pullulan+3.5‰ sildenafil)
Absorbance [a.u.]
1800
1750
1700
1650
1600
1550
1500
Wavenumbers [cm-1]

Figure 8

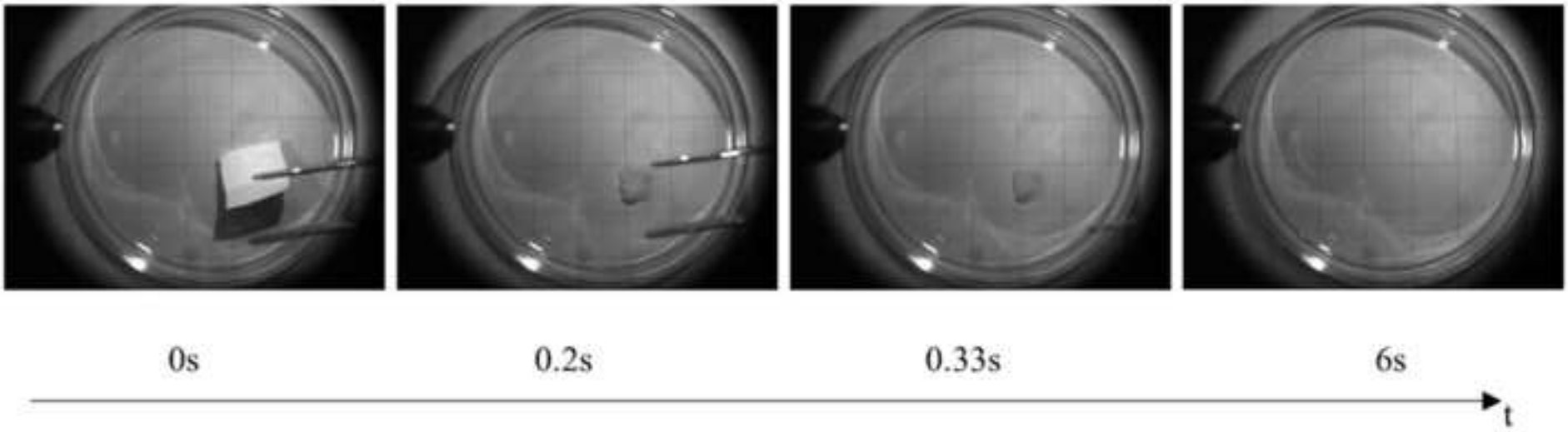

Figure 9

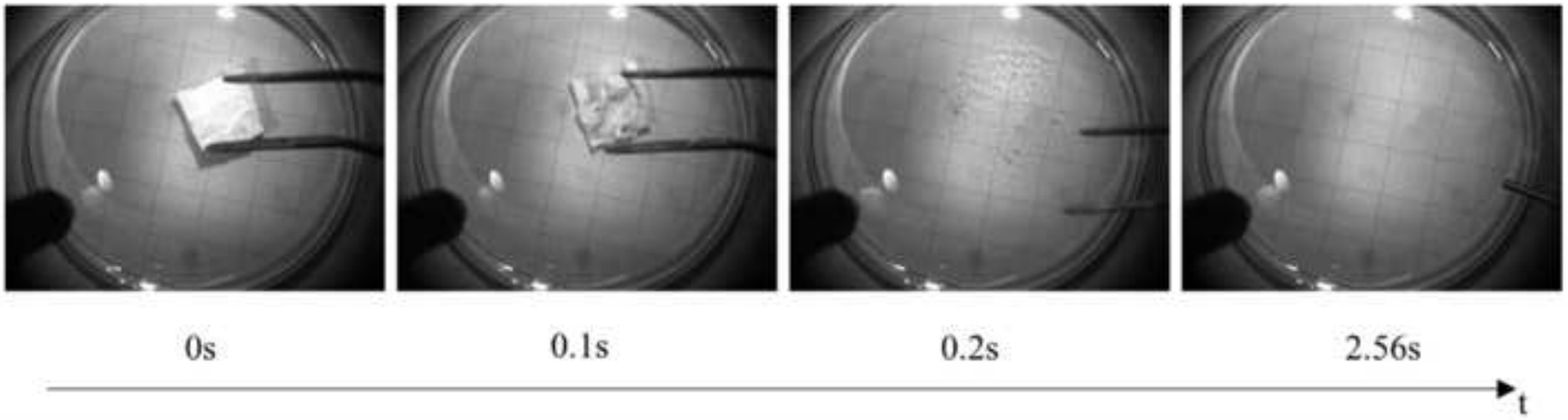

Figure S1: zero shear viscosity of solutions containing 20%wt of pullulan and increasing amounts of sildenafil (2‰wt, 2.5‰wt, 3‰wt, 3.5‰wt)

Figure S2: photograph taken at the optical microscope (5x magnification) highlighting the effect of dripping during electrospinning of the solution containing 20%wt of pullulan and 3.5‰wt of sildenafil (operating conditions: 16kV, 4.0mL/h, 200mm TCD, 22.4°C and RH 27%)

Figure S3: SEM photographs highlighting the effect of residual water content (possibly combined with electrostatic effect) during electrospinning of the solution containing 20%wt of pullulan and saturated with sildenafil (operating conditions: 20kV, 1.0mL/h, 200mm TCD, 21.7°C and RH 32%).

Figure S1 - Supplementary Material

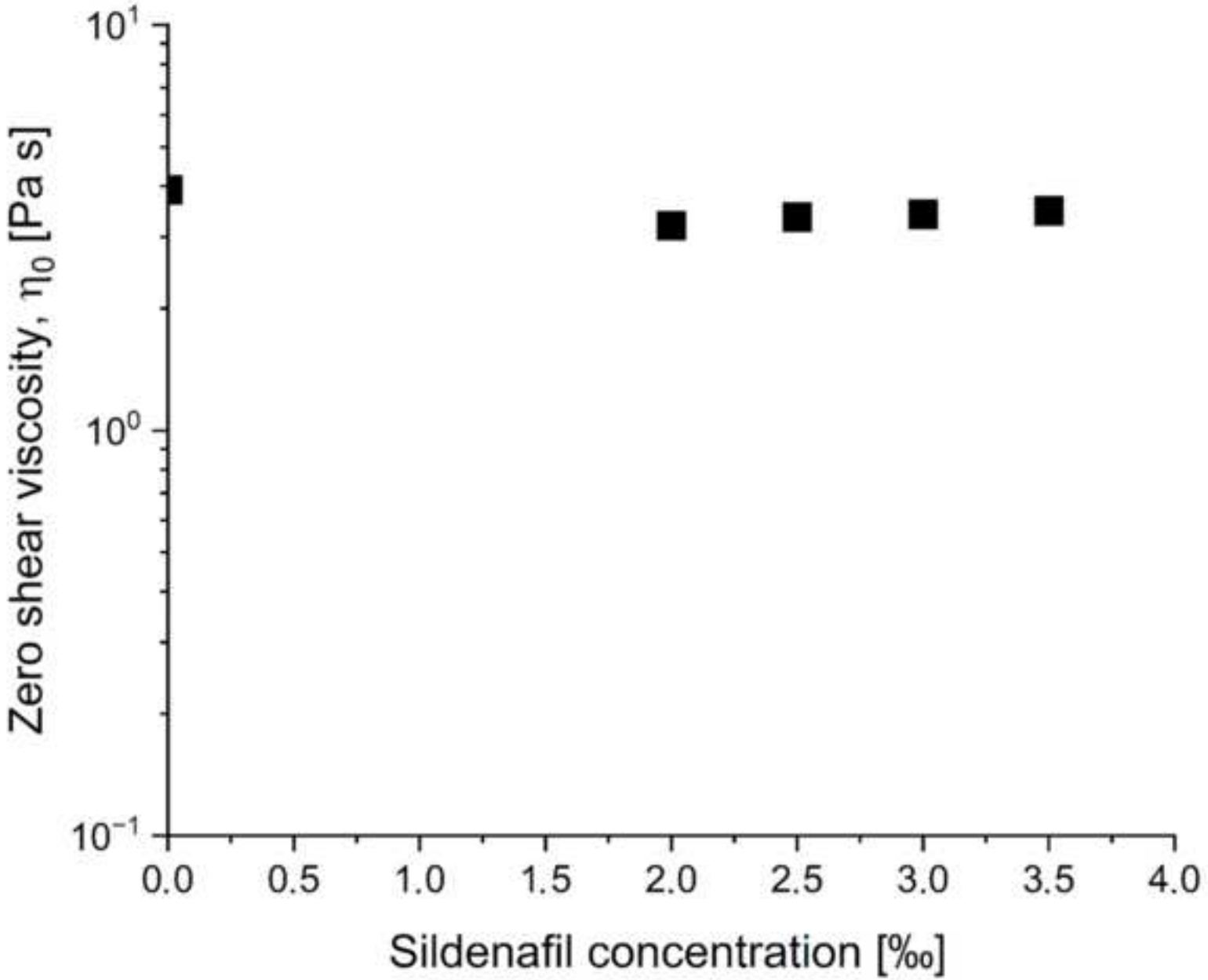

Figure S2 - Supplementary Material

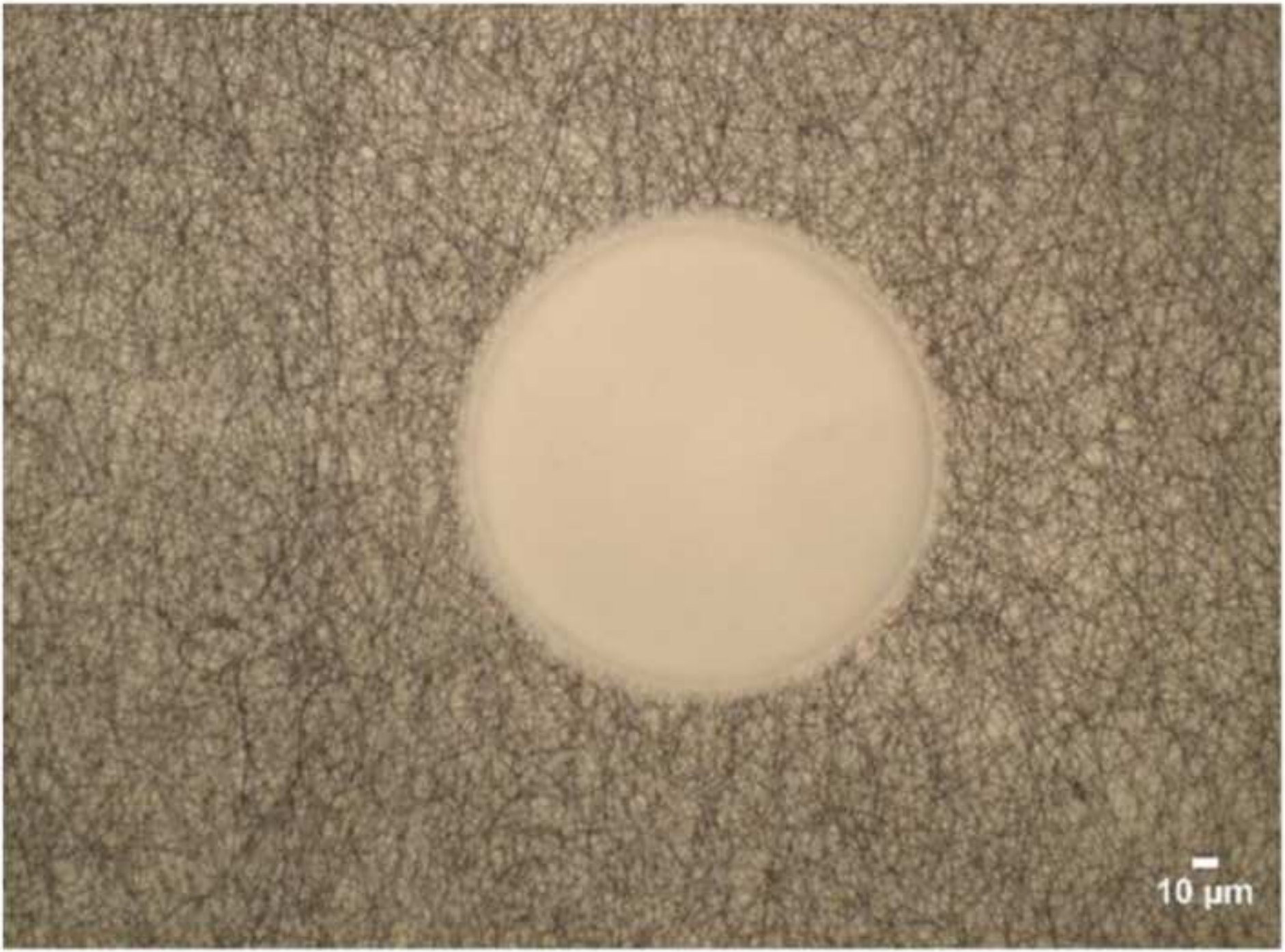

Figure S3 - Supplementary Material

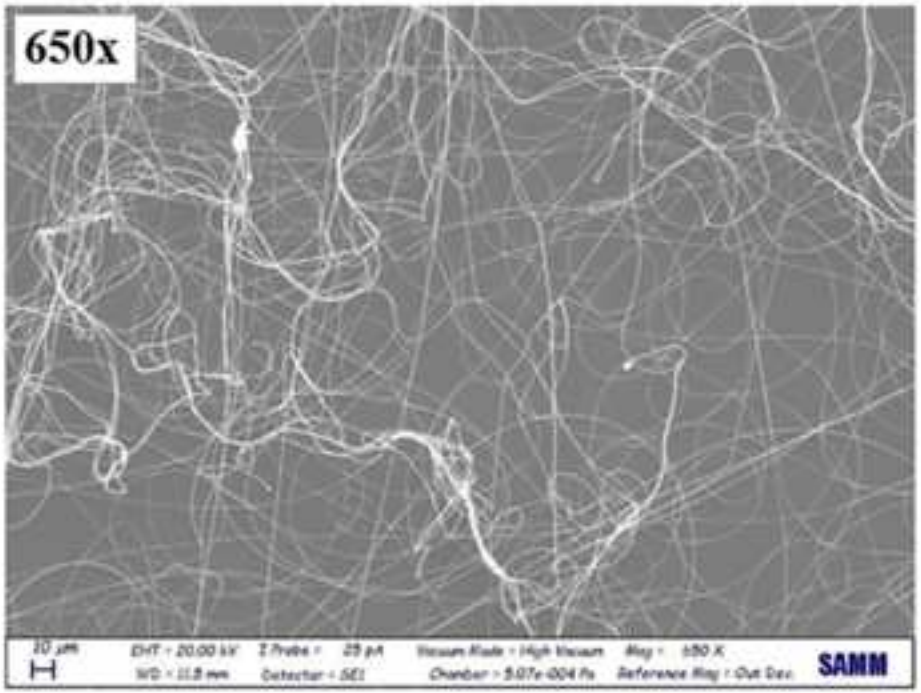

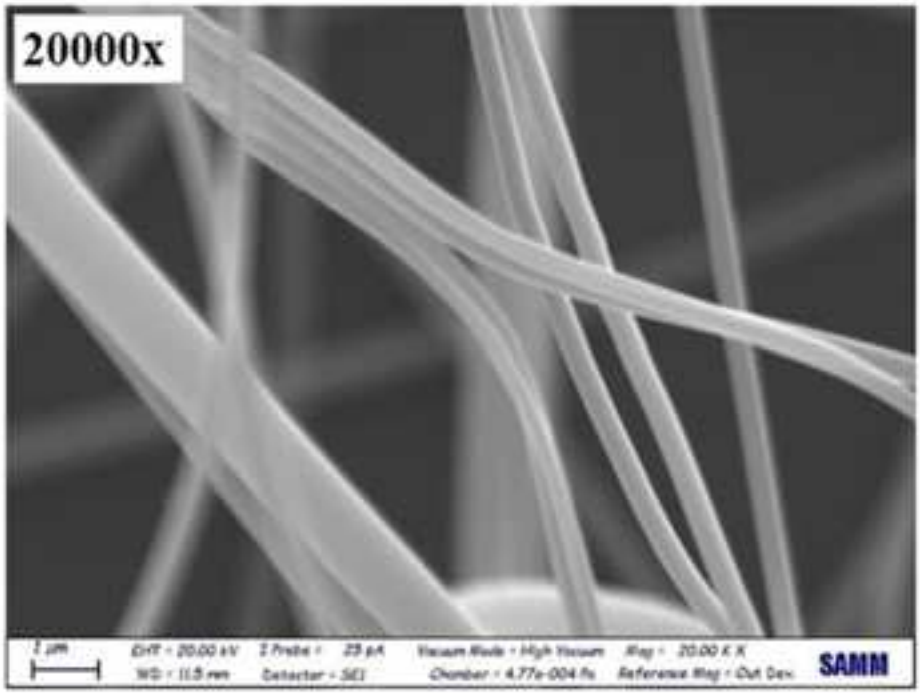

Click here to access/download

Video Still

Ravasi E. et al., Video S4.mp4

Click here to access/download

Video Still

Ravasi E. et al., Video S5.mp4